Title: Childhood obesity is linked to putative neuroinflammation in brain white matter, hypothalamus, and striatum

Authors: Zhaolong Li, BA[1, 2], Amjad Samara, MD[1, 3], Mary Katherine Ray, PhD[1], Jerrel Rutlin, BS[1], Cyrus A. Raji, MD, PhD[3, 4], Joshua S. Shimony, MD, PhD[4], Peng Sun, PhD[4, a], Sheng-Kwei Song, PhD[4], Tamara Hershey, PhD[1, 2, 3, 4], Sarah A. Eisenstein, PhD[1, 4, *]

Affiliations:
[1]Department of Psychiatry, Washington University School of Medicine, St. Louis, MO 63110
[2]Department of Psychological and Brain Sciences, Washington University in St. Louis, St. Louis, MO 63130
[3]Department of Neurology, Washington University School of Medicine, St. Louis, St. Louis, MO 63110
[4]Mallinckrodt Institute of Radiology, Washington University School of Medicine, St. Louis, MO 63110
[a]Present address: Department of Imaging Physics, University of Texas MD Anderson Cancer Center, Houston, TX 77030

Running title: Brain tissue microstructure in children with obesity

***Corresponding author**:
Sarah A. Eisenstein, PhD
Associate Professor, Department of Psychiatry
Washington University School of Medicine
St. Louis, MO 63110
Campus Box 8134
Phone: (314)-362-7107
Email: seisens@wustl.edu

Abstract

Introduction

Childhood obesity is increasingly prevalent and confers elevated risk of developing medical complications across the lifespan. Given the brain's prominent involvement in homeostatic and hedonic eating, it is crucial to understand brain health in obesity. Recent studies using quantitative T2-weighted MRI and diffusion-weighted MRI showed obesity-related putative neuroinflammation in human brain. To assess convergent validity across diffusion-based MRI techniques and extend these findings, this study characterized tissue microstructure of white matter (WM) tracts and energy regulation and reward processing brain regions in children across levels of obesity-related measures, using diffusion basis spectrum imaging (DBSI).

Methods

Using data from the Adolescent Brain Cognitive Development℠ Study (ABCD Study®), DBSI metrics indicative of putative neuroinflammation were computed for WM tracts, hypothalamus, nucleus accumbens, caudate nucleus, and putamen. DBSI metrics were compared between children with normal-weight vs. obesity. DBSI metrics were also correlated to baseline and one- and two-year change in continuous obesity-related measures (waist circumference, BMI, and BMI *z*-scores). Striatal DBSI findings were compared to those of restriction spectrum imaging (RSI).

Results

A total of 263 nine- and ten-year old children from the ABCD Study® 2.0.1 data release (5 underweight; 126 with normal-weight; 64 with over-weight; 68 with obesity) who met inclusion and exclusion criteria were randomly selected. Relative to children with normal-weight, children with obesity had lower DBSI fiber fraction (FF; reflects apparent axonal/dendritic density) and higher DBSI restricted fraction (RF; reflects cellularity) in WM tracts throughout the brain (voxel-wise FWE-corrected $p < 0.05$), as well as higher DBSI-RF in the hypothalamus, nucleus accumbens, and caudate nucleus (Cohen's d's ≥ 0.28, p's ≤ 0.05). Across all children, greater baseline waist circumference was related to higher DBSI-RF in the hypothalamus (standardized $\beta = 0.17$, $p = 0.0033$), nucleus accumbens (standardized $\beta = 0.21$, $p = 0.0001$), and caudate nucleus (standardized $\beta = 0.14$, $p = 0.013$). Gain in waist circumference over one and two years related to higher baseline DBSI-RF in nucleus accumbens (standardized $\beta = 0.12$, $p = 0.08$) and in hypothalamus (standardized $\beta = 0.15$, $p = 0.03$), respectively. Overall, results were consistent for BMI and BMI *z*-scores. Similar results were observed using RSI metrics.

Conclusion

Novel findings include demonstration that, as in adults, childhood obesity is associated with DBSI-assessed putative neuroinflammation in WM tracts and hypothalamus. In addition, our results support the reproducibility of previous findings that MRI-assessed putative neuroinflammation in striatum and hypothalamus is related to obesity in children, contributing to a growing understanding of the role of adiposity in brain health across the lifespan.

Keywords: childhood obesity; neuroinflammation; white matter; hypothalamus; nucleus accumbens; diffusion basis spectrum imaging (DBSI).

Abbreviations

ABCD®, Adolescent Brain Cognitive Development℠; ADC, apparent diffusion coefficient; AUC, area-under-the-curve; BMI, body mass index; CI, confidence interval; DBSI, diffusion basis spectrum imaging; DWI, diffusion-weighted images; FF, fiber fraction; FWE, family-wise error; ICV, intracranial volume; MRI, magnetic resonance imaging; NW, children with normal-weight; OB, children with obesity; OW, children with over-weight; PDS, pubertal development scale; RF, restricted fraction; ROI, region of interest; RSI, restriction spectrum imaging; SD, standard deviation; SE, standard error; SES, socioeconomic status; TBSS, tract-based spatial statistics; VIF, variance inflation factor; WC, waist circumference; WM, white matter

1. Introduction

Obesity is a major, growing health issue in youth (Hales et al., 2020; Ng et al., 2014). It is associated with higher medical costs (Biener et al., 2020), lower reported quality of life (Killedar et al., 2020), greater psychological concerns (e.g., depression, anxiety) (Wang & Veugelers, 2008), and higher risk of current and future medical complications such as adult obesity, type 2 diabetes, cardiovascular disease, and stroke (Liang et al., 2015; Must & Strauss, 1999; Simmonds et al., 2016). There is also accumulating evidence that childhood obesity is linked to cognitive dysfunction and elevated risk for developing Alzheimer's disease in late-life (Tait et al., 2022). Compromised health in childhood obesity, along with the brain's prominent role in regulation of feeding and metabolism, makes understanding the relationship between obesity-related measures (including waist circumference and body mass index (BMI)) and brain health essential. Determining which brain regions and circuits play a role in development and maintenance of childhood obesity may inform risk assessments and targets for obesity intervention and prevention, thereby mitigating both short- and long-term health consequences.

Obesity is a disease of chronic, low-grade, systemic inflammation with widespread effects on multiple organs (Gregor & Hotamisligil, 2011). In rodent models of diet-induced obesity, short- and long-term high-fat or Western diets induce inflammation in the central nervous system, or "neuroinflammation" (Baufeld et al., 2016; Buckman et al., 2013; De Souza et al., 2005), which in turn causes memory impairment (Beilharz et al., 2016; Pistell et al., 2010). In humans, post-mortem brain tissue analyses have shown associations between obesity and increased gliosis in multiple brain regions, including the hypothalamus, a key regulator of feeding and metabolism (Baufeld et al., 2016; Schur et al., 2015).

Investigating obesity-related neuroinflammation in living humans, however, requires non-invasive methods, such as brain magnetic resonance imaging (MRI)-based assessments. Diffusion basis spectrum imaging (DBSI) (Cross & Song, 2017), a diffusion MRI-based technique applied to diffusion-weighted images to model anisotropic and isotropic water diffusivities separately within tissue microstructure (Wang et al., 2011; White et al., 2013), has been histopathologically validated as neuroinflammation-sensitive using rodent and human neural tissue in multiple sclerosis (Chiang et al., 2014; Wang et al., 2014; Wang et al., 2011, 2015), epilepsy (Zhan et al., 2018), and optic neuritis (Lin et al., 2017; Yang et al., 2021). DBSI-assessed putative neuroinflammation in white matter (WM) correlates with cerebrospinal fluid biomarkers in Alzheimer's disease (Wang et al., 2019). Using DBSI, we have observed putative neuroinflammatory processes including cellularity, vasogenic edema, and lower apparent axonal and dendritic densities in white matter (WM) tracts, striatal, and limbic regions in adults with obesity (Samara et al., 2020, 2021). DBSI has not yet been used to assess obesity-related putative neuroinflammation in children. However, Rapuano et al. (2020) used the diffusion-based MRI technique restriction spectrum imaging (RSI), which, in contrast to DBSI, models isotropic water diffusion components based on the ratio of radial and axial anisotropic water diffusivities (Palmer et al., 2022; White et al., 2013), and observed that greater purported cellular density in striatal and limbic regions relates to greater baseline and future waist circumference and BMI metrics in children enrolled in the Adolescent Brain Cognitive Development^{SM} Study (ABCD Study®) (Casey et al., 2018; Rapuano et al., 2020, 2022). Also, using a non-diffusion MRI-based method of assessing putative neuroinflammation, namely quantitative T2-weighted MRI, studies have reported that longer hypothalamic T2 relaxation times and greater T2 signal intensity, both suggestive of reactive microglial and astrocytic gliosis normally seen in response to brain injury, relate to higher BMI in adults (Schur et al., 2015; Thaler et al., 2012) and children, including a subset enrolled in the ABCD Study® (Sewaybricker et al., 2019;

Sewaybricker, Kee, et al., 2021; Sewaybricker, Melhorn, et al., 2021). Convergent findings amongst MRI methods in the same participants would support the feasibility and reliability of these techniques to assess obesity-related putative neuroinflammation in children.

In this study, we leveraged the open-source data from the ABCD Study®, randomly selecting a power analysis-informed subsample of nine- and ten-year old children stratified by sex and BMI category, to test the primary hypotheses that 1) DBSI-assessed obesity-related neuroinflammation we observed in WM tracts and striatal regions in adults is also present in children, and 2) the DBSI metric for cellularity, namely restricted fraction (DBSI-RF), relates to waist circumference and BMI metrics in children in a robust manner similar to the RSI metric for cellular density, namely restricted isotropic component, in striatal regions as well as two novel regions unexamined in children using diffusion-based MRI modeling, hypothalamus and WM tracts. If our results in striatal regions and hypothalamus are similar to those in studies that used RSI and quantitative T2-weighted methods, respectively, they will support the use of non-invasive MRI-based techniques to measure obesity-related putative neuroinflammation *in vivo* in humans, in the absence of histopathologic validation.

2. Material and methods

2.1. Participants

Participants were selected from the ABCD Study®, a ten-year, longitudinal, observational, multi-site study on brain development in a diverse cohort of U.S. children and adolescents with an open data-sharing policy (Casey et al., 2018; Compton et al., 2019; Garavan et al., 2018; Jernigan et al., 2018). In the ABCD Study ®, physical, cognitive, social, emotional, environmental, behavioral, and academic assessments are administered annually, and neuroimaging and bioassays are performed biennially. Details of recruitment, design, and exclusion criteria of the study have been reported elsewhere (Garavan et al., 2018). Institutional review boards at participating study sites approved study procedures. Parents gave written consent and children gave verbal assent.

The ABCD Study® 2.0.1 release included baseline data from 11,875 participants and 4,951 participants at one-year follow-up. Participants who had history of neurological disorders (cerebral palsy, epilepsy), traumatic brain injury, schizophrenia and substance use disorder were excluded from the ABCD Study®. Similar to Rapuano et al. (2020), the present analysis further excluded participants with history of schizophrenia, attention-deficit hyperactivity disorder, autism spectrum disorder, diabetes, lead poisoning, muscular dystrophy, and multiple sclerosis. Also in line with Rapuano et al. (2020), only scans performed on Siemens 3T Prisma machines (Siemens Healthineers AG, Erlangen, Germany) were included. A total of 1,962 participants met these additional inclusion and exclusion criteria, had complete baseline T1-weighted and diffusion-weighted MRI that passed quality control, and had both baseline and one-year follow-up anthropometric data. Additionally, anthropometric data at two-year follow-up was obtained from the ABCD Study® 4.0 release.

2.1.1. Power analysis

We analyzed a subsample of the qualifying 1,962 participants in order to streamline analyses. Based on previously reported effect sizes for obesity-related neuroinflammation assessed by DBSI (Cohen's d's ≥ 0.7) (Samara et al., 2021), RSI (Cohen's d's ~ 0.5) (Rapuano et al., 2020), and quantitative T2-weighted MRI (Cohen's d's ≥ 0.65) (Sewaybricker et al., 2019; Sewaybricker, Melhorn, et al., 2021), a sample size of 140 would provide 0.8 statistical power at $\alpha = 0.05$ to detect obesity-related neuroinflammation as assessed by DBSI. To better ensure sufficient power, which is often overestimated in power analyses, we first randomly selected 200 participants. As participants with over-weight (OW)

and obesity (OB) were underrepresented in this initial selection (OW, n = 22; OB, n = 28; for definitions of groups see **section 2.2**), an additional 50 OW and 50 OB participants were randomly selected, stratified by sex. The addition of data from 100 additional participants in OW and OB groups was technically feasible and, based on the power analyses, should provide sufficient power to detect the primary outcomes of interest, i.e., relationships between DBSI-assessed putative neuroinflammation in striatum, hypothalamus and WM tracts and obesity-related measures. The sample (n = 300) consisted of 7 children with underweight, 143 with normal-weight (NW), 72 OW, and 78 OB (prior to neuroimage processing; see **section 2.1.2**).

2.1.2. Final sample

After diffusion-weighted image (DWI) preprocessing, data from 19 participants (2 underweight, 11 NW, 2 OW, 4 OB) were excluded due to missing/incomplete DWI acquisition, missing field maps, mismatch between field map and DWI dimensions, or missing/unclear DWI directions. Greater mean head motion during MRI acquisition was marginally correlated with higher baseline BMI *z*-scores (p = 0.09) (**Supplementary Fig. 1**). Upon visual inspection, motion was clearly above normal (> 2.5 mm) for 11 participants (3 NW, 4 OW, 4 OB); these participants were excluded (for detailed rationale, see **section 2.3.2**). Data from two participants who had missing baseline pubertal development scale (PDS) scores was excluded. Additionally, five participants (2 NW, 2 OW, 1 OB) had erroneous hypothalamus segmentations and were excluded. The final sample therefore consisted of 5 underweight, 126 NW, 64 OW, and 68 OB (total n = 263).

2.2. Obesity-related measures and groups

Participants had measurements of waist circumference (in), weight, and height from baseline and one- and two-year follow-up visits (Barch et al., 2018). Raw BMIs (kg/m^2) were calculated. BMI *z*-scores adjusted for age and sex were computed using the 2000 CDC growth charts (https://www.cdc.gov/nccdphp/dnpao/growthcharts/resources/sas.htm) (Kuczmarski et al., 2002). These different measures were used to address the concern that a single measure may be less related to obesity-related putative neuroinflammation than others. Baseline BMI percentiles (computed at https://www.cdc.gov/healthyweight/bmi/calculator.html) were used to group participants (but were not used as continuous measures in regression due to ceiling at 100th percentile), defined as children with underweight (BMI < 5th percentile), NW (5th to < 85th percentiles), OW (85th to < 95th percentiles), and OB (≥ 95th percentile) (Kuczmarski et al., 2002).

2.3. Neuroimaging analyses

2.3.1. MRI acquisition

Details on baseline MRI scanning and T1 and diffusion-weighted sequences and data harmonization across sites have been reported elsewhere (Casey et al., 2018; Hagler et al., 2019). Briefly, spin echo echo-planar imaging (EPI) was used to acquire diffusion-weighted images (DWI) with the following parameters: total acquisition time = 7:31, repetition time (TR) = 4100 ms, time to echo (TE) = 88 ms, matrix size = 140 × 140 × 81, flip angle = 90°, and voxel resolution = 1.7 mm^3 isotropic. DWI were acquired in the axial plane with 96 gradient directions (b = 500 s/mm^2, 6 directions; 1,000 s/mm^2, 15 directions; 2,000 s/mm^2, 15 directions; 3,000 s/mm^2, 60 directions; and 7 b = 0 frames).

2.3.2. DWI and DBSI processing

DWI preprocessing steps included susceptibility-induced distortion correction using field maps (*topup*), brain extraction (*BET*), and eddy currents and participant motion correction (*eddy*), all using the FMRIB Software Library (FSL) tools (Smith et al., 2004).

Diffusion basis spectrum imaging (DBSI) multi-tensor maps were estimated using an in-house MATLAB script as previously described (Wang et al., 2011, 2015). DBSI assesses brain tissue microstructure by modeling both isotropic and anisotropic water diffusion within each voxel in white and grey matter. DBSI yielded maps of anisotropic fiber fraction (DBSI-FF; reflects apparent axonal/dendritic density); isotropic nonrestricted fraction (DBSI-NRF; *f*(D) at ADC > 0.3 μm^2/ms; reflects vasogenic edema/tissue disintegration/extracellular water); and isotropic restricted fraction (DBSI-RF; *f*(D) at 0 < ADC ≤ 0.3 μm^2/ms; reflects intracellular water/inflammation-related cellularity) (Chiang et al., 2014; Sun et al., 2020; Wang et al., 2015). Importantly, DBSI-FF and RF are consistently and robustly lower and greater, respectively, in adults with obesity relative to adults with normal-weight (Samara et al., 2020, 2021) and serve as the neuroinflammation-related independent variables in the current study. DBSI maps were then registered to T1 anatomical space, first using FSL *epi_reg* and a non-diffusion weighted (b0) image, and then by applying the resultant transformation matrix to individual maps using FSL *applyxfm*.

Participant head motion during MRI acquisition is known to interfere with diffusion tensor fitting and yield spurious correlations (Ling et al., 2012; Power et al., 2012; Yendiki et al., 2014). Moreover, greater motion is behaviorally and genetically linked to higher BMI (Hodgson et al., 2017). To control for this, in addition to distortion correction during DWI preprocessing, participants with high mean head motion (> 2.5 mm, calculated as mean framewise displacement during DWI scans) were excluded, and mean head motion was included as a covariate in all analyses.

2.3.3. White matter tract-based spatial statistics (TBSS)

Voxel-wise analyses of WM DBSI-FF and RF were performed using TBSS (Smith et al., 2006). Diffusion tensor imaging (DTI) tensors were fitted to preprocessed DWI using FSL *dtifit*. To remove outliers from DTI fitting, DTI fractional anisotropy (FA) images were slightly eroded by one voxel, and end slices were removed. Cleaned DTI-FA images were then nonlinearly registered to the recommended FMRIB58-FA standard-space image, averaged, and assigned a threshold at FA > 0.2 to create a WM skeleton. DBSI-FF and RF value maps were projected onto the WM skeleton.

2.3.4. Subcortical ROI segmentation

The nucleus accumbens, caudate nucleus, and putamen regions-of-interest (ROIs) were segmented from T1-weighted structural images using FSL's *FIRST* tool (Patenaude et al., 2011). Prior to statistical analysis, all segmentations were visually inspected for accuracy. For each ROI, volume and mean DBSI-FF and RF metrics were each extracted and combined/averaged between hemispheres.

2.3.5. Hypothalamus segmentation

Protocols for participant selection and analyses involving the hypothalamus were preregistered at DOI: 10.17605/OSF.IO/FB5WS. Briefly, the hypothalamus was segmented using a novel, fully automated, validated algorithm developed on deep convolutional neural networks (Billot et al., 2020). To assess the accuracy of this algorithm in children, 20 randomly selected T1-weighted images (10 NW and 10 OB) underwent both automated and manual hypothalamus segmentation. The manual segmentation followed the same atlas the automated algorithm was trained on (Makris et al., 2013). Within this sub-cohort, spatial overlap (assessed using Dice similarity coefficient with acceptable value ≥ 0.7) and volumetric correlation between automated and manual segmentations were assessed. Furthermore, these Dice similarity coefficients and volumetric correlations were compared between NW and OB sub-cohorts to uncover any group differences in segmentation.

Within the sub-cohort of 20 participants, the mean Dice similarity coefficient between automated and manual hypothalamus segmentations was higher than the acceptable 0.7 (*mean* = 0.735, *SD* = 0.018; $p = 2.8 \times 10^{-8}$) and was not different between NW and OB sub-cohorts ($p = 0.58$). Hypothalamus volumes

were highly correlated between automated and manual segmentations, both in the total sub-cohort (r = 0.74, p = 0.0002) (**Supplementary Fig. 2A**) and within OB and NW sub-cohorts (p = 0.018 and 0.005); the correlations did not differ by BMI category (p = 0.97). Although automated segmentations yielded smaller volumes than manual segmentations (*mean* = 747 and 887 mm^3; $p = 9.1 \times 10^{-5}$), such volume reduction mainly excluded voxels bordering the hypothalamus and neighboring tissue (**Supplementary Fig. 2B**), mitigating possible partial-volume effects. Also, the segmented volumes were similar to literature values (Neudorfer et al., 2020). Taken together, the automated algorithm reliably produced hypothalamus segmentations relative to manual segmentation. Prior to statistical analysis, all hypothalamus segmentations were visually inspected for accuracy. Volume and mean DBSI-FF and RF metrics were each extracted and combined/averaged between hemispheres.

2.4. Statistical analyses

All statistical analyses, except for TBSS (see **section 2.3.3**), were performed in R version 4.1.1 (R Core Team, 2013).

2.4.1. Group comparisons and regression modeling

Missing demographic data at baseline were imputed using the "mice" R package (van Buuren & Groothuis-Oudshoorn, 2011) and included 20 entries for income. Differences in demographic and obesity-related measures across different BMI categories were assessed using one-way analysis of variance (ANOVA) or chi-square tests. For regression relating baseline DBSI metrics to obesity-related measures at one-year, imputed data included 17 entries for income. For regression relating baseline DBSI metrics to obesity-related measures at two-year, imputed data included 19 entries for income. Pairwise deletion was applied to subcortical DBSI outliers (± 3SD from mean; **Supplementary Table 1)** in individual analyses. Sample size ranges for each set of analyses are reported under the corresponding **Supplementary Tables 2-7**.

Baseline DBSI-FF and RF in WM tracts were compared between NW (n = 126) and OB (n = 68) groups on a voxel-wise basis using TBSS general linear models with covariates of age, sex, race/ethnicity, parental education, pubertal development scale (PDS) scores and mean head motion during MRI acquisition. FSL *Randomize* (null distribution built from 5000 permutations; threshold-free cluster enhancement (TFCE)) was used for these comparisons with spatial family-wise error (FWE) rate corrected $p < 0.05$) (Winkler et al., 2014). Briefly, the raw statistical image was TFCE-transformed into an output image in which voxel-wise TFCE scores were weighted sums of local clustered signals, such that larger TFCE scores reflected magnitude of cluster-like spatial support greater than a given height (signal intensity) (Li et al., 2017; Smith & Nichols, 2009). We specified the –T2 option in *Randomize* (2D optimization for skeletonized data, cluster height weighted by H = 2, cluster extent weighted by E = 1, voxel connectivity = 26). Relative to group mean comparisons, voxel-wise analyses using TBSS and TFCE allow for sensitive detection of regionally-specific group differences in DBSI metrics in WM tracts while stringently controlling for multiple comparisons across space.

Baseline DBSI metrics from subcortical grey matter ROIs were compared between NW and OB groups using analysis of covariance (ANCOVA). Covariates included participant age, sex, race/ethnicity, parental education, PDS score, mean head motion during MRI acquisition, and estimated total intracranial volume (ICV). We had *a priori* directional hypotheses for each test and statistical significance was defined at family-wise error $\alpha = 0.05 / [4 \text{ ROIs}] = 0.0125$. For each comparison, we calculated adjusted group means and standard errors (SEs), as well as Cohen's d with 95% confidence interval (CI) for effect sizes.

To assess the association between DBSI metrics and continuous obesity-related measures (e.g., BMI ranging from underweight to obesity) while addressing study site as a random effect, linear mixed effects models (Bates et al., 2015) were applied to relate either baseline or one-year and two-year change in obesity-related measures to baseline DBSI metrics of each ROI. All models included fixed effects of participant age (at baseline, one- or two-year), sex, race/ethnicity, PDS score (at baseline, one- or two-year), parental education, household income, parental marital status, mean head motion, ICV, and corresponding baseline obesity-related measures. Family structure was not covaried as only four families included related individuals (two each) in our dataset. As we had *a priori* hypotheses, and the goal was to describe ROI-specific obesity-related putative neuroinflammation and likely convergent obesity-related measures, significance was thresholded with each ROI treated as a family, at $\alpha = 0.0125$. Model *p*-values were estimated using Satterthwaite's method (Kuznetsova et al., 2017). Standardized β regression coefficients with 95% CI and partial R^2 were calculated for effect sizes. Quality control for linear mixed effects models included checking normality of residuals, homoscedasticity, and multicollinearity.

2.4.2. DBSI and RSI comparison

RSI restricted isotropic component from the nucleus accumbens, caudate nucleus, and putamen was extracted from the ABCD Study® dataset (Hagler et al., 2019). The ABCD Study® segmented ROIs using FreeSurfer v5.3 (instead of FSL's *FIRST* as in our DBSI processing); the hypothalamus was not specifically segmented or analyzed and voxel-wise data for WM tracts was not available. Associations between RSI restricted component and baseline and one- and two-year change in obesity-related measures were evaluated using linear mixed effects models, as described for DBSI in **section 2.4.1**. RSI defines putative neuroinflammation as an increase in restricted (intracellular water diffusivity) component. To further compare model performance, DBSI-RF and RSI restricted component were tested to classify NW and OB participants using logistic regression, controlling for participant age, sex, race/ethnicity, parental education, PDS scores, mean head motion, and ICV. These covariates were identical to those used in group comparisons (**section 2.4.1**). Receiver operating characteristic (ROC) curves and area-under-the-curve (AUC) were computed using the "pROC" package (Robin et al., 2011).

3. Results

3.1. Participant information

Demographics, ICV and subcortical ROI volumes, and obesity-related measures are described in **Table 1**. Mean motion did not differ significantly between groups from different BMI categories. Groups also did not differ significantly in ROI volumes; these volumes were thus not covaried separately from ICV in analyses. For reference, distributions for baseline obesity-related measures are shown in **Supplementary Fig. 3**.

3.2. Comparison of DBSI metrics in WM tracts between NW and OB groups

Voxel-wise analysis using TBSS suggested that relative to NW ($n = 126$), the OB ($n = 68$) group had significantly lower DBSI-FF (reflecting axonal/dendritic density) and higher DBSI-RF (reflecting cellularity) throughout WM tracts (all FWE-corrected $p < 0.05$) (**Fig. 1**).

3.3. Comparison of DBSI metrics in subcortical ROIs between NW and OB groups

Compared to NW ($n = 126$), the OB ($n = 68$) group had higher DBSI-RF in the nucleus accumbens and, at significance levels that did not survive multiple comparisons correction, caudate nucleus and hypothalamus (**Fig. 2, Table 2**). DBSI-RF in the putamen did not differ between OB and NW groups. Groups did not differ on DBSI-FF in any of the ROIs (**Table 2**).

3.4. Association between DBSI in subcortical ROIs and continuous obesity-related measures

3.4.1. Baseline waist circumference, BMI, and BMI *z*-scores

Across all 263 participants (underweight, NW, OW, and OB), greater baseline waist circumference was significantly associated with greater DBSI-RF in the hypothalamus, nucleus accumbens, and caudate nucleus. The putamen demonstrated a similar association though did not survive multiple comparison correction (**Fig. 3A**). In these analyses, mean head motion was not a significant covariate (all p's ≥ 0.05). All results were consistent when BMI and BMI *z*-scores were used as dependent measures (**Supplementary Fig. 4;** tabulated statistics in **Supplementary Table 2**).

Additionally, greater baseline BMI *z*-scores related to lower DBSI-FF, or putative dendritic density, in the hypothalamus ($p = 0.0014$, **Supplementary Fig. 5A**). Although not surviving multiple comparison correction, greater baseline BMI *z*-scores related to lower DBSI-FF in the putamen ($p = 0.047$**, Supplementary Fig. 5B**). All other associations were not significant (all p's ≥ 0.06; **Supplementary Table 2**).

When quality control determined that distribution assumptions were violated in linear mixed effects models, variables were log or *z*-transformed as appropriate. However, as linear mixed effects models are robust to assumption violations (Schielzeth et al., 2020), analyses using transformed fixed effects and/or dependent variables yielded similar results in magnitude and direction to those with non-transformed variables and did not influence statistical significance. Continuous model predictors typically had variance inflation factor (VIF) < 2.5, suggesting independence from each other.

Linear mixed effects regression models typically explained 20-30% of the variance in baseline obesity-related measures; for example, the model relating baseline waist circumference to DBSI-RF in the hypothalamus had full $R^2 = 0.211$, and the model relating baseline BMI *z*-scores to DBSI-RF in the nucleus accumbens had full $R^2 = 0.289$. Differences between models were largely due to the different DBSI metrics in different ROIs being investigated. DBSI-RF uniquely explained 2.1% (putamen), 2.6% (caudate nucleus), 3.3% (hypothalamus), and 6.0% (nucleus accumbens) of variance in baseline obesity-related measures (**Fig. 3B**). Beyond DBSI, higher parental education (high school diploma and/or some college), higher PDS scores (reflective of more advanced pubertal stage), and larger ICV tended to associate with greater baseline obesity-related measures (e.g., in the model relating baseline waist circumference to DBSI-RF in the nucleus accumbens, p's = 0.002, 0.005, and 0.027, respectively; partial R^2's = 0.095, 0.053, and 0.018, respectively).

3.4.2. One- and two-year change in waist circumference, BMI, and BMI *z*-scores

In 250-251 children with complete data, baseline DBSI-RF in the nucleus accumbens tended to predict one-year gain in waist circumference and BMI when accounting for corresponding baseline obesity-related measures, though these results were trend-level. As the current study sample size was not powered to detect weaker effects observed in Rapuano et al. (2020), our results, although at trend-level *p*-values, are of note and shown in **Fig. 4A**. No other significant associations were observed (**Supplementary Table 3**). In 247-248 children with complete data, baseline DBSI-RF in the hypothalamus predicted two-year gain in waist circumference when baseline waist circumference was accounted for (**Fig. 4B**). Other changes in obesity-related measures at two-year follow-up were not predicted by baseline DBSI neuroinflammation-related metrics (**Supplementary Table 4**).

Significant predictors of gain in waist circumference or BMI metrics tended to include larger ICV, female sex, and higher PDS scores (e.g., in the modeling relating one-year change in waist circumference to baseline nucleus accumbens DBSI-RF, p's = 0.020, 0.024, 0.028 and partial R^2's = 0.020, 0.019, and 0.018, respectively). Baseline levels of waist circumference and BMI metrics were also

important predictors of their respective future changes (e.g., in the three models discussed above, p's ≤ 0.08 and partial R^2's ≥ 0.12).

3.5. Association between RSI in subcortical ROIs and continuous obesity-related measures

3.5.1. Baseline waist circumference, BMI, and BMI *z*-scores

Standardized β coefficients with 95% CI, p-values, and partial R^2 for RSI metrics are shown in **Supplementary Table 5.** Greater baseline waist circumference was associated with higher RSI restricted component in the nucleus accumbens. Results were the same for BMI and BMI *z*-scores. Associations for the caudate nucleus and putamen were less strong overall as evidenced by smaller effect sizes with p-values at trend-level or not surviving multiple comparisons correction.

3.5.2. One- and two-year change in waist circumference, BMI, and BMI *z*-scores

Standardized β coefficients with 95% CI, p-values, and partial R^2 for RSI metrics are shown in **Supplementary Table 6 and 7.** Higher baseline RSI restricted component in the nucleus accumbens was related, though not surviving multiple comparison correction, to one-year gain in BMI *z*-scores when accounting for baseline levels. No strong associations were observed for caudate nucleus or putamen. No associations were found for two-year changes in obesity-related measures.

3.6. Comparison between DBSI and RSI on classifying NW and OB groups

Metrics reflective of neuroinflammation-related cellularity from DBSIRF and RSI restricted component showed similar sensitivity and specificity in classifying NW and OB participants (**Fig. 5**). For both techniques, metrics from the nucleus accumbens classified groups marginally better than those from caudate nucleus or putamen. Across the striatum, DBSI-RF correlated positively with RSI restricted component (Pearson's r's ≥ 0.35, p's ≤ 6.2×10^{-9}) (**Supplementary Fig. 6**).

4. Discussion

4.1. Overview and significance

Here we present both novel findings and support for the rigor and reproducibility of previous neuroimaging studies that observed obesity-associated putative neuroinflammation in key feeding and reward processing brain regions as assessed by MRI in children and adults. First, using a different diffusion MRI-based model of putative neuroinflammation (i.e., DBSI) than Rapuano et al. (2020) (i.e., RSI), we show that greater putative cellularity in the nucleus accumbens relates to greater waist circumference, BMI and BMI *z*-scores in < 300 randomly selected 9- and 10-year-old children enrolled in the ABCD Study®, the sample size of which was based on larger effect sizes detected in the Rapuano et al. (2020) report that included thousands of children. The effect sizes of the relationships between nucleus accumbens DBSI-RF and obesity-related measures are remarkably similar to those seen with RSI restricted component as in Rapuano et al. (2020), demonstrating that these observations are robust and reliable across diffusion MRI methods. The convergence between the findings reported here and by Rapuano et al. (2020) support the sensitivity and utility of diffusion-based MRI techniques in detecting putative neuroinflammation in obesity.

Second, we observed relationships between obesity-related measures and putative neuroinflammation in two brain regions, WM tracts and hypothalamus, that were not assessed by Rapuano et al. (2020). Our results in the hypothalamus are in line with previous reports of putative gliosis in the mediobasal hypothalamus, as assessed by quantitative T2 MRI, in both adults and children with obesity, although effects in striatal or other limbic regions were not observed in these studies (Schur et al., 2015; Sewaybricker et al., 2019; Sewaybricker, Kee, et al., 2021; Sewaybricker, Melhorn, et al., 2021; Thaler et al., 2012). Here, our findings both add to evidence for obesity-related putative

neuroinflammation in the hypothalamus in children and support the reliability of both non-diffusion and diffusion-based MRI methods for assessing obesity-related neuroinflammation, although the former appears to be specific to putative gliosis in the mediobasal hypothalamus.

Third, to our knowledge, this study is the first to investigate and report obesity-related neuroinflammation in WM tracts in children, in line with our previous studies of DBSI-assessed neuroinflammation in white matter tracts in adults (Samara et al., 2020) and supporting DBSI as a method that is sensitive to putative neuroinflammation across different age groups. Together, our findings and those in previous studies indicate that young children manifest obesity-related differences in brain microstructure, which may affect current and future susceptibility for weight gain and its comorbidities including cognitive impairment, type 2 diabetes, and late-life dementia.

4.2. Links between obesity, neuroinflammation, and brain function

The highly vascularized hypothalamus responds to and transmits signals from feeding-related hormones, neuronal signals, and nutrients derived from the bloodstream (Velloso & Schwartz, 2011). As a “metabolic sensor”, the hypothalamus is vulnerable to overfeeding and obesity-related elevations in levels of plasma pro-inflammatory mediators including cytokines and saturated fatty acids (Lieu et al., 2021). Overfeeding also causes the blood-brain barrier to break down, further enabling inflammatory factors to access the central nervous system (Guillemot-Legris et al., 2016; Guillemot-Legris & Muccioli, 2017; Stranahan et al., 2016). Our finding that DBSI-assessed cellularity (DBSI-RF) in the hypothalamus is greater in childhood obesity is consistent with the recruitment, proliferation, and morphological transformation of astrocytes and microglia (i.e., reactive gliosis) and elevated cytokine expression seen in this brain regions of rodents fed with chronic high-fat diets (Gómez-Apo et al., 2021; Milanski et al., 2009). While initial activation of astrocytes and microglia may be neuroprotective, chronic low-grade activation leads to harmful neuroinflammatory processes that disrupt hypothalamic metabolic regulation and contribute to overfeeding, leptin and insulin-resistance, and development of obesity (Gómez-Apo et al., 2021; Macedo et al., 2019; Sochocka et al., 2017).

The striatum plays a key role in reward processing and appetitive behavior (Maldonado-Irizarry et al., 1995; Stice et al., 2011). Striatal activity, predominantly dopamine neurotransmission, is informed by homeostatic signals from the hypothalamus and by feeding-related hormones, both acting on receptors on midbrain dopaminergic cells (Abizaid et al., 2006; Figlewicz et al., 2003; Figlewicz, 2016; Hommel et al., 2006; King et al., 2011; Krügel et al., 2003; Naleid et al., 2005; Skibicka et al., 2011). There is evidence suggesting altered dopamine neurotransmission in obesity (Geiger et al., 2009; Wang et al., 2001; Wu et al., 2017). Beyond hypothalamic influences, neuroinflammation in the striatum may further contribute to obesogenic behavior. Indeed, our observation of DBSI-assessed cellularity (DBSI-RF) in the striatum in children with obesity is consistent with diet-induced reactive gliosis in the nucleus accumbens of juvenile and adult rodents (Décarie-Spain et al., 2018; Molina et al., 2020). Furthermore, the association between baseline nucleus accumbens cellularity and future weight gain, as observed by us and others (Rapuano et al., 2020, 2022), relates to striatal neuroinflammation-mediated overfeeding in rodent studies (Décarie-Spain et al., 2018). Interestingly, we previously found that putative neuroinflammation in the nucleus accumbens mediates the relationship between obesity and greater self-reported emotional eating in adults (Samara et al., 2021) and Rapuano et al. (2022) recently observed that greater putative cellular density in this region mediates the relationship between greater dietary fat intake and higher waist circumference and BMI in children. Taken together, the MRI-based assessments of the hypothalamus and striatum by our lab and others are consistent and report putative neuroinflammation in these regions in childhood obesity, in agreement with studies in rodent models and human adults.

4.3. Neuroinflammation in childhood vs. adult obesity

Overall, the pattern of our results in children agrees with previous DBSI assessments of obesity-related neuroinflammation in adults (Ly et al., 2021; Samara et al., 2020, 2021). Patterns in apparent axonal/dendritic density (DBSI-FF) and cellularity (DBSI-RF) were spatially widespread in WM tracts in both adults and in children in the current study. However, in subcortical regions, adults and children differ in the patterns observed. For example, children with obesity had higher cellularity (DBSI-RF) in the nucleus accumbens than children with normal-weight, but no such difference was observed in adults. Differences in scanner site and diffusion-weighted MRI sequence parameters across adults and children make interpretation of these differences difficult. To determine whether diffusion-weighted MRI-based neuroinflammation metrics differ in magnitude or quality between childhood and adult obesity, matched MRI scanners and sequences and, optimally, longitudinal study designs are necessary. Fortunately, by performing MRI scans in the same participants biennially from childhood through adolescence and adulthood, the ABCD Study® may provide a future opportunity for performing a sufficiently powered longitudinal investigation of MRI-assessed obesity-related neuroinflammation and general microstructure over development.

It remains an open question whether our findings in adults and children indicate time-dependent changes or developmental differences in obesity-related neuroinflammation. It is possible that putative cellularity and gliosis effects seen in children constitute early reactive responses to obesity-associated neuroinflammation that precede more substantial downstream vasogenic edema and tissue loss seen in adults (Dorrance et al., 2014; Prieto et al., 2014; Raji et al., 2010; Sochocka et al., 2017), as in multiple sclerosis (Kamholz & Garbern, 2005). Furthermore, as executive control regions such as the prefrontal cortex mature later in adolescence relative to the striatum (Spear, 2000), neuroinflammation in the striatum may be more strongly linked to obesity and/or obesogenic behavior in childhood than in adult obesity. Of note, a recent study found that RSI restricted component in the striatum increases with age in normally-developing children, though the study did not control for adiposity (Palmer et al., 2022). Future longitudinal research on both subcortical and cortical brain regions is needed to test any time or development-related effects.

4.4. Comparison between DBSI and RSI findings

Although DBSI and RSI differ in their derivation of putative neuroinflammation metrics, their restricted fraction or component measures have been interpreted similarly such that the isotropic intracellular water fraction is thought to reflect the degree of neuroinflammation-related immune cell infiltration or tissue cellularity. Indeed, in the current study, DBSI- and RSI-assessed cellularity in the striatum related similarly with obesity-related measures and strongly with each other, and classified obesity status with comparable performance. If these metrics did not reflect similar properties in tissue microstructure, our small sample size, based on effect sizes of the primary RSI findings (Rapuano et al., 2020), would have either lacked power to detect significant relationships between DBSI-RF and obesity-related measures, or we might have observed associations between DBSI-RF and obesity-related measures different in direction and/or magnitude. In general, the agreeing findings between DBSI and RSI highlight that diffusion MRI-based techniques are sensitive to and useful for characterizing obesity-associated neuroinflammation in children, adding a novel neuroimaging tool to existing modalities that assess putative neuroinflammation such as quantitative T2-weighted MRI.

4.5. Strengths and limitations

The current study had strengths and limitations. We took advantage of the large, racially and socioeconomically diverse dataset in the ABCD Study® to power an analysis of diffusion MRI-assessed

putative neuroinflammation in WM tracts, hypothalamus, and striatum and its relation to baseline and future waist circumference and BMI metrics in nine and ten-year old children. Further, the T1 and diffusion-weighted MRI sequences used in the ABCD Study® were optimized for high spatial resolution, which likely contributed to our ability to detect microstructural variations in terms of regional water diffusivity across children in different BMI categories. Optimal T1-weighted structural MRI also significantly contributed to our rigorous test of automated vs. labor-intensive, traditional manual segmentations of the hypothalamus. The results from this test substantiated our confidence in reliably segmenting this region and isolating its diffusion signal from partial volume effects that may occur due to its small size, heavy vascularization, and extensive neighboring of heterogenous tissue. Finally, we show that head motion during MRI acquisition that related to greater waist circumference and BMI metrics did not significantly confound the association between neuroimaging metrics and obesity-related metrics, thereby alleviating concerns of undue influence by motion on our results.

Limitations and future directions include, first, the lack of future time points besides one- and two-year follow-ups, at which to assess both neuroimaging and obesity-related measures. It is possible that neuroinflammation, which in weight gain and obesity may be a chronic yet subtle process, affects clinical and behavioral outcomes on a time scale larger than two years. Also, as the ABCD Study® does not record obesity duration, we could not assess when and to what extent neuroinflammation occurs relative to obesity onset. Future research tracking any children moving from normal-weight to obesity would be useful. Second, the current study only compared DBSI and RSI. Using other diffusion-weighted MRI techniques, such as neurite orientation dispersion and density imaging (NODDI) (Zhang et al., 2012) and diffusion kurtosis imaging (DKI) (Steven et al., 2013), to characterize tissue microstructure and its relation to obesity-related measures in the ABCD Study® dataset may offer additional insight, though it is of interest to note DBSI might offer better accuracy in small fiber crossing angles and edema (Ye et al., 2021). Third, since the focus of the current study was on assessing neuroinflammation in feeding-related brain regions and its association with obesity-related measures, factors including socioeconomic status (SES) and puberty that likely impact child development, though controlled for in analyses, were unexplored. These factors warrant further investigation. As **Table 1** shows, there was uneven racial distributions across SES factors and BMI categories, and it is crucial to investigate how SES and obesity-related measures interact to affect neuroinflammation and brain health during development (Dennis et al., 2022).

Our smaller sample size was powered to determine whether DBSI could detect the robust effects found using RSI in Rapuano et al. (2020), specifically, obesity-related putative cellularity (DBSI-RF) in striatal regions. In Rapuano et al. (2020, 2022), effect sizes were noticeably smaller for the prediction of *future* waist circumference and BMI metrics by RSI restricted component in nucleus accumbens compared to baseline results. It should be noted that all data from the children in the current study were included in that of Rapuano et al. (2020), making up 5% of the previous study's baseline sample size. Therefore, we likely lacked power to detect significant relationships between DBSI-RF and future waist circumference or BMI metrics. In addition, to avoid further ambiguity in interpretation of trend-level or non-significant results due to Type II error, we did not investigate DBSI-assessed neuroinflammation in other regions included in Rapuano et al. (2020) (thalamus, pallidum, hippocampus, amygdala, ventral diencephalon), which had less robust obesity-associated putative neuroinflammation as assessed by RSI. Therefore, it remains to be determined whether DBSI acts similar to RSI in these regions.

Finally, the largest limitation of the current study is the limited interpretation of diffusion-weighted MRI neuroinflammation metrics. While DBSI-assessed neuroinflammation metrics have been

histopathologically validated in some inflammatory neurological diseases including human multiple sclerosis (Wang et al., 2015), rodent models of multiple sclerosis (Chiang et al., 2014; Wang et al., 2011), and rodent optic neuritis (Lin et al., 2017; Yang et al., 2021), this is not the case for obesity. The validity of DBSI and RSI neuroinflammation metrics as true reflections of obesity-related cellularity and/or gliosis remains to be proven using histopathology in post-mortem brains of individuals that, ideally, were recently neuroimaged, or in animal models of obesity. On a related note, it is difficult to determine whether key feeding regions, including hypothalamus and nucleus accumbens, are uniquely involved in obesity-related neuroinflammation because a true control region in which this phenomenon is definitively non-existent has not been identified. Alternatively, in adults, confidence in the face validity of MRI-based measures of obesity-related neuroinflammation may be increased by corroborating MRI findings within individuals using positron emission tomography (PET) with radioligands that bind to neuroinflammatory indicators including astrocytes and microglia.

4.6. Conclusions and implications

With DBSI, we observed putative neuroinflammation in WM tracts, hypothalamus, and striatum in children with obesity. Agreement between DBSI and RSI suggested that diffusion-weighted MRI is a sensitive and useful tool for assessing obesity-related cellularity in children. Given that rapid and substantial developmental processes occur during childhood and adolescence, further work is needed to elucidate how obesity-related neuroinflammation may independently and jointly with these processes contribute to obesity and comorbidities during these periods (Dietz, 1994). Longitudinal studies will help uncover long-term functional impacts of neuroinflammation on clinical and behavioral outcomes in childhood obesity.

Funding: This work was supported by the National Institutes of Health (NIH) Grants (R01DK085575 (TH), T32DA007261-29 (AS, MKR, SAE), 1RF1AG072637-01 (CAR)), WUSTL NIH KL2 Grant (KL2TR000450 – ICTS Multidisciplinary Clinical Research Career Development Program (MKR, CAR)), WUSTL Diabetes Research Center Pilot & Feasibility Award (P30 DK020579 (SAE)), Neuroimaging Laboratory Research Center Innovation Matching Funds (SAE), the Radiological Society of North America Research Scholar Grant (CAR), the Mallinckrodt Institute of Radiology Pilot Award (SAE), the Mallinckrodt Institute of Radiology Summer Research Program (ZL), the Washington University Summer Undergraduate Research Award (ZL), Clinical and Translational Science Award (UL1TR000448), WUSTL Intellectual and Developmental Disabilities Research Center (PHD103525), and WUSTL McDonnell Center for Systems Neuroscience. The ABCD Study® is supported by the NIH and federal partners (awards U01DA041048, U01DA050989, U01DA051016, U01DA041022, U01DA051018, U01DA051037, U01DA050987, U01DA041174, U01DA041106, U01DA041117, U01DA041028, U01DA041134, U01DA050988, U01DA051039, U01DA041156, U01DA041025, U01DA041120, U01DA051038, U01DA041148, U01DA041093, U01DA041089, U24DA041123, and U24DA041147). A full list of supporters is available at https://abcdstudy.org/federal-partners.html. This work was supported by funds provided by the McDonnell Center for Systems Neuroscience at Washington University in St. Louis. The funders had no role in study design, data collection and analysis, decision to publish, or preparation of the manuscript. The content is solely the responsibility of the authors and does not necessarily represent the official views of the National Institutes of Health.

Declaration of interest: The authors declare no conflict of interest.

Author contributions (CRediT): Zhaolong Li, BA: Conceptualization, Methodology, Formal analysis, Writing – Original & Draft, Writing – Review & Editing, Visualization; **Amjad Samara, MD:** Conceptualization, Formal analysis, Writing – Review & Editing, Visualization; **Mary Katherine Ray, PhD:** Conceptualization, Formal analysis, Writing – Original & Draft, Writing – Review & Editing; **Jerrel Rutlin, BS:** Software, Methodology; **Cyrus A. Raji, MD, PhD:** Methodology; **Joshua S. Shimony, MD, PhD:** Methodology, Writing – Review & Editing; **Peng Sun, PhD:** Software, Methodology; **Sheng-Kwei Song, PhD:** Software, Methodology, Writing – Review & Editing; **Tamara Hershey, PhD:** Conceptualization, Methodology, Writing – Review & Editing, Supervision; **Sarah A. Eisenstein, PhD:** Conceptualization, Methodology, Formal analysis, Validation, Writing – Original & Draft, Writing – Review & Editing, Supervision

Acknowledgements: The authors wish to thank Richard Ni, Jonathan Koller, and Heather Lugar for their assistance with neuroimaging analyses in this study.

Data availability statement: The ABCD Study® data are publicly available through the National Institute of Mental Health Data (NIDA) Archive (https://nda.nih.gov/abcd). The ABCD Study® data used in this report came from The ABCD Study® Data Release 4.0 (DOI: 10.15154/1523041, October 2021).

References

Abizaid, A., Liu, Z.-W., Andrews, Z. B., Shanabrough, M., Borok, E., Elsworth, J. D., Roth, R. H., Sleeman, M. W., Picciotto, M. R., Tschöp, M. H., Gao, X.-B., & Horvath, T. L. (2006). Ghrelin modulates the activity and synaptic input organization of midbrain dopamine neurons while promoting appetite. *The Journal of Clinical Investigation*, *116*(12), 3229–3239. https://doi.org/10.1172/JCI29867

Barch, D. M., Albaugh, M. D., Avenevoli, S., Chang, L., Clark, D. B., Glantz, M. D., Hudziak, J. J., Jernigan, T. L., Tapert, S. F., Yurgelun-Todd, D., Alia-Klein, N., Potter, A. S., Paulus, M. P., Prouty, D., Zucker, R. A., & Sher, K. J. (2018). Demographic, physical and mental health assessments in the adolescent brain and cognitive development study: Rationale and description. *Developmental Cognitive Neuroscience*, *32*, 55–66. https://doi.org/https://doi.org/10.1016/j.dcn.2017.10.010

Bates, D., Mächler, M., Bolker, B., & Walker, S. (2015). Fitting Linear Mixed-Effects Models Using lme4. *Journal of Statistical Software; Vol 1, Issue 1 (2015)* . https://www.jstatsoft.org/v067/i01

Baufeld, C., Osterloh, A., Prokop, S., Miller, K. R., & Heppner, F. L. (2016). High-fat diet-induced brain region-specific phenotypic spectrum of CNS resident microglia. *Acta Neuropathologica*, *132*(3), 361–375. https://doi.org/10.1007/s00401-016-1595-4

Beilharz, J. E., Maniam, J., & Morris, M. J. (2016). Short-term exposure to a diet high in fat and sugar, or liquid sugar, selectively impairs hippocampal-dependent memory, with differential impacts on inflammation. *Behavioural Brain Research*, *306*, 1–7. https://doi.org/https://doi.org/10.1016/j.bbr.2016.03.018

Biener, A. I., Cawley, J., & Meyerhoefer, C. (2020). The medical care costs of obesity and severe obesity in youth: An instrumental variables approach. *Health Economics*, *29*(5), 624–639. https://doi.org/https://doi.org/10.1002/hec.4007

Billot, B., Bocchetta, M., Todd, E., Dalca, A. V., Rohrer, J. D., & Iglesias, J. E. (2020). Automated segmentation of the hypothalamus and associated subunits in brain MRI. *NeuroImage*, *223*, 117287. https://doi.org/10.1016/j.neuroimage.2020.117287

Buckman, L. B., Thompson, M. M., Moreno, H. N., & Ellacott, K. L. J. (2013). Regional astrogliosis in the mouse hypothalamus in response to obesity. *Journal of Comparative Neurology*, *521*(6), 1322–1333. https://doi.org/https://doi.org/10.1002/cne.23233

Casey, B. J., Cannonier, T., Conley, M. I., Cohen, A. O., Barch, D. M., Heitzeg, M. M., Soules, M. E., Teslovich, T., Dellarco, D. V, Garavan, H., Orr, C. A., Wager, T. D., Banich, M. T., Speer, N. K., Sutherland, M. T., Riedel, M. C., Dick, A. S., Bjork, J. M., Thomas, K. M., … Dale, A. M. (2018). The Adolescent Brain Cognitive Development (ABCD) study: Imaging acquisition across 21 sites. *Developmental Cognitive Neuroscience*, *32*, 43–54. https://doi.org/https://doi.org/10.1016/j.dcn.2018.03.001

Chiang, C. W., Wang, Y., Sun, P., Lin, T. H., Trinkaus, K., Cross, A. H., & Song, S. K. (2014). Quantifying white matter tract diffusion parameters in the presence of increased extra-fiber cellularity and vasogenic edema. *NeuroImage*, *101*, 310–319. https://doi.org/10.1016/j.neuroimage.2014.06.064

Compton, W. M., Dowling, G. J., & Garavan, H. (2019). Ensuring the Best Use of Data: The Adolescent Brain Cognitive Development Study. *JAMA Pediatrics*, *173*(9), 809–810. https://doi.org/10.1001/jamapediatrics.2019.2081

Cross, A. H., & Song, S. K. (2017). "A new imaging modality to non-invasively assess multiple sclerosis pathology." *Journal of Neuroimmunology*, *304*, 81–85. https://doi.org/10.1016/j.jneuroim.2016.10.002

De Souza, C. T., Araujo, E. P., Bordin, S., Ashimine, R., Zollner, R. L., Boschero, A. C., Saad, M. J. A., & Velloso, L. A. (2005). Consumption of a fat-rich diet activates a proinflammatory response and induces insulin resistance in the hypothalamus. *Endocrinology*, *146*(10), 4192–4199. https://doi.org/10.1210/en.2004-1520

Décarie-Spain, L., Sharma, S., Hryhorczuk, C., Issa-Garcia, V., Barker, P. A., Arbour, N., Alquier, T., & Fulton, S. (2018). Nucleus accumbens inflammation mediates anxiodepressive behavior and compulsive sucrose seeking elicited by saturated dietary fat. *Molecular Metabolism*, *10*, 1–13. https://doi.org/10.1016/j.molmet.2018.01.018

Dennis, E., Manza, P., & Volkow, N. D. (2022). Socioeconomic status, BMI, and brain development in children. *Translational Psychiatry*, *12*(1), 33. https://doi.org/10.1038/s41398-022-01779-3

Dietz, W. H. (1994). Critical periods in childhood for the development of obesity. *The American Journal of Clinical Nutrition*, *59*(5), 955–959. https://doi.org/10.1093/ajcn/59.5.955

Dorrance, A. M., Matin, N., & Pires, P. W. (2014). The effects of obesity on the cerebral vasculature. *Current Vascular Pharmacology*, *12*(3), 462–472. https://doi.org/10.2174/1570161112666140423222411

Figlewicz, D P, Evans, S. B., Murphy, J., Hoen, M., & Baskin, D. G. (2003). Expression of receptors for insulin and leptin in the ventral tegmental area/substantia nigra (VTA/SN) of the rat. *Brain Research*, *964*(1), 107–115. https://doi.org/https://doi.org/10.1016/S0006-8993(02)04087-8

Figlewicz, Dianne P. (2016). Expression of receptors for insulin and leptin in the ventral tegmental area/substantia nigra (VTA/SN) of the rat: Historical perspective. *Brain Research*, *1645*, 68–70. https://doi.org/https://doi.org/10.1016/j.brainres.2015.12.041

Garavan, H., Bartsch, H., Conway, K., Decastro, A., Goldstein, R. Z., Heeringa, S., Jernigan, T., Potter, A., Thompson, W., & Zahs, D. (2018). Recruiting the ABCD sample: Design considerations and procedures. *Developmental Cognitive Neuroscience*, *32*, 16–22. https://doi.org/10.1016/j.dcn.2018.04.004

Geiger, B. M., Haburcak, M., Avena, N. M., Moyer, M. C., Hoebel, B. G., & Pothos, E. N. (2009). Deficits of mesolimbic dopamine neurotransmission in rat dietary obesity. *Neuroscience*, *159*(4), 1193–1199. https://doi.org/https://doi.org/10.1016/j.neuroscience.2009.02.007

Gómez-Apo, E., Mondragón-Maya, A., Ferrari-Díaz, M., & Silva-Pereyra, J. (2021). Structural Brain Changes Associated with Overweight and Obesity. *Journal of Obesity*, *2021*, 6613385. https://doi.org/10.1155/2021/6613385

Gregor, M. F., & Hotamisligil, G. S. (2011). Inflammatory Mechanisms in Obesity. *Annual Review of Immunology*, *29*(1), 415–445. https://doi.org/10.1146/annurev-immunol-031210-101322

Guillemot-Legris, O., Masquelier, J., Everard, A., Cani, P. D., Alhouayek, M., & Muccioli, G. G. (2016). High-fat diet feeding differentially affects the development of inflammation in the central nervous system. *Journal of Neuroinflammation*, *13*(1), 206. https://doi.org/10.1186/s12974-016-0666-8

Guillemot-Legris, O., & Muccioli, G. G. (2017). Obesity-Induced Neuroinflammation: Beyond the Hypothalamus. In *Trends in Neurosciences* (Vol. 40, Issue 4, pp. 237–253). Elsevier Ltd. https://doi.org/10.1016/j.tins.2017.02.005

Hagler, D. J., Hatton, S., Cornejo, M. D., Makowski, C., Fair, D. A., Dick, A. S., Sutherland, M. T., Casey, B. J., Barch, D. M., Harms, M. P., Watts, R., Bjork, J. M., Garavan, H. P., Hilmer, L., Pung, C. J., Sicat, C. S., Kuperman, J., Bartsch, H., Xue, F., … Dale, A. M. (2019). Image processing and analysis methods for the Adolescent Brain Cognitive Development Study. *NeuroImage*, *202*, 116091. https://doi.org/https://doi.org/10.1016/j.neuroimage.2019.116091

Hales, C., Carroll, M., Fryar, C., & Ogden, C. (2020). *Prevalence of obesity and severe obesity among adults: United States, 2017–2018*.

Hodgson, K., Poldrack, R. A., Curran, J. E., Knowles, E. E., Mathias, S., Göring, H. H. H., Yao, N., Olvera, R. L., Fox, P. T., Almasy, L., Duggirala, R., Barch, D. M., Blangero, J., & Glahn, D. C. (2017). Shared Genetic Factors Influence Head Motion During MRI and Body Mass Index. *Cerebral Cortex (New York, N.Y. : 1991)*, *27*(12), 5539–5546. https://doi.org/10.1093/cercor/bhw321

Hommel, J. D., Trinko, R., Sears, R. M., Georgescu, D., Liu, Z.-W., Gao, X.-B., Thurmon, J. J., Marinelli, M., & DiLeone, R. J. (2006). Leptin Receptor Signaling in Midbrain Dopamine Neurons Regulates Feeding. *Neuron*, *51*(6), 801–810. https://doi.org/10.1016/j.neuron.2006.08.023

Jernigan, T. L., Brown, S. A., & Dowling, G. J. (2018). The Adolescent Brain Cognitive Development Study. *Journal of Research on Adolescence : The Official Journal of the Society for Research on Adolescence*, *28*(1), 154–156. https://doi.org/10.1111/jora.12374

Kamholz, J. A., & Garbern, J. Y. (2005). Neuronal cell injury precedes brain atrophy in multiple sclerosis. *Neurology*, *64*(1), 176 LP – 176. https://doi.org/10.1212/WNL.64.1.176

Killedar, A., Lung, T., Petrou, S., Teixeira-Pinto, A., Tan, E. J., & Hayes, A. (2020). Weight status and health-related quality of life during childhood and adolescence: effects of age and socioeconomic position. *International Journal of Obesity*, *44*(3), 637–645. https://doi.org/10.1038/s41366-020-0529-3

King, S. J., Isaacs, A. M., O'Farrell, E., & Abizaid, A. (2011). Motivation to obtain preferred foods is enhanced by ghrelin in the ventral tegmental area. *Hormones and Behavior*, *60*(5), 572–580. https://doi.org/https://doi.org/10.1016/j.yhbeh.2011.08.006

Krügel, U., Schraft, T., Kittner, H., Kiess, W., & Illes, P. (2003). Basal and feeding-evoked dopamine release in the rat nucleus accumbens is depressed by leptin. *European Journal of Pharmacology*, *482*(1), 185–187. https://doi.org/https://doi.org/10.1016/j.ejphar.2003.09.047

Kuczmarski, R. J., Ogden, C. L., Guo, S. S., Grummer-Strawn, L. M., Flegal, K. M., Mei, Z., Wei, R., Curtin, L. R., Roche, A.

F., & Johnson, C. L. (2002). 2000 CDC Growth Charts for the United States: methods and development. *Vital and Health Statistics. Series 11, Data from the National Health Survey*, *246*, 1–190.

Kuznetsova, A., Brockhoff, P. B., & Christensen, R. H. B. (2017). lmerTest Package: Tests in Linear Mixed Effects Models. *Journal of Statistical Software*, *82*(13 SE-Articles), 1–26. https://doi.org/10.18637/jss.v082.i13

Li, H., Nickerson, L. D., Nichols, T. E., & Gao, J.-H. (2017). Comparison of a non-stationary voxelation-corrected cluster-size test with TFCE for group-Level MRI inference. *Human Brain Mapping*, *38*(3), 1269–1280. https://doi.org/https://doi.org/10.1002/hbm.23453

Liang, Y., Hou, D., Zhao, X., Wang, L., Hu, Y., Liu, J., Cheng, H., Yang, P., Shan, X., Yan, Y., Cruickshank, J. K., & Mi, J. (2015). Childhood obesity affects adult metabolic syndrome and diabetes. *Endocrine*, *50*(1), 87–92. https://doi.org/10.1007/s12020-015-0560-7

Lieu, C. V, Loganathan, N., & Belsham, D. D. (2021). Mechanisms Driving Palmitate-Mediated Neuronal Dysregulation in the Hypothalamus. *Cells*, *10*(11). https://doi.org/10.3390/cells10113120

Lin, T.-H., Chiang, C.-W., Perez-Torres, C. J., Sun, P., Wallendorf, M., Schmidt, R. E., Cross, A. H., & Song, S.-K. (2017). Diffusion MRI quantifies early axonal loss in the presence of nerve swelling. *Journal of Neuroinflammation*, *14*(1), 78. https://doi.org/10.1186/s12974-017-0852-3

Ling, J., Merideth, F., Caprihan, A., Pena, A., Teshiba, T., & Mayer, A. R. (2012). Head injury or head motion? Assessment and quantification of motion artifacts in diffusion tensor imaging studies. *Human Brain Mapping*, *33*(1), 50–62. https://doi.org/10.1002/hbm.21192

Ly, M., Raji, C. A., Yu, G. Z., Wang, Q., Wang, Y., Schindler, S. E., An, H., Samara, A., Eisenstein, S. A., Hershey, T., Smith, G., Klein, S., Liu, J., Xiong, C., Ances, B. M., Morris, J. C., & Benzinger, T. L. S. (2021). Obesity and White Matter Neuroinflammation Related Edema in Alzheimer's Disease Dementia Biomarker Negative Cognitively Normal Individuals. *Journal of Alzheimer's Disease*, *79*, 1801–1811. https://doi.org/10.3233/JAD-201242

Macedo, F., dos Santos, L. S., Glezer, I., & da Cunha, F. M. (2019). Brain Innate Immune Response in Diet-Induced Obesity as a Paradigm for Metabolic Influence on Inflammatory Signaling . In *Frontiers in Neuroscience* (Vol. 13, p. 342). https://www.frontiersin.org/article/10.3389/fnins.2019.00342

Makris, N., Swaab, D. F., van der Kouwe, A., Abbs, B., Boriel, D., Handa, R. J., Tobet, S., & Goldstein, J. M. (2013). Volumetric parcellation methodology of the human hypothalamus in neuroimaging: Normative data and sex differences. *NeuroImage*, *69*, 1–10. https://doi.org/https://doi.org/10.1016/j.neuroimage.2012.12.008

Maldonado-Irizarry, C. S., Swanson, C. J., & Kelley, A. E. (1995). Glutamate receptors in the nucleus accumbens shell control feeding behavior via the lateral hypothalamus. *The Journal of Neuroscience*, *15*(10), 6779 LP – 6788. https://doi.org/10.1523/JNEUROSCI.15-10-06779.1995

Milanski, M., Degasperi, G., Coope, A., Morari, J., Denis, R., Cintra, D. E., Tsukumo, D. M. L., Anhe, G., Amaral, M. E., Takahashi, H. K., Curi, R., Oliveira, H. C., Carvalheira, J. B. C., Bordin, S., Saad, M. J., & Velloso, L. A. (2009). Saturated fatty acids produce an inflammatory response predominantly through the activation of TLR4 signaling in hypothalamus: implications for the pathogenesis of obesity. *The Journal of Neuroscience : The Official Journal of the Society for Neuroscience*, *29*(2), 359–370. https://doi.org/10.1523/JNEUROSCI.2760-08.2009

Molina, J., Joaquim, A., Bonamin, L. V., Martins, M. de F. M., Kirsten, T. B., Cardoso, C. V., Bernardi, M. M., & Bondan, E. F. (2020). Reduced astrocytic expression of GFAP in the offspring of female rats that received hypercaloric diet. *Nutritional Neuroscience*, *23*(6), 411–421. https://doi.org/10.1080/1028415X.2018.1512783

Must, A., & Strauss, R. S. (1999). Risks and consequences of childhood and adolescent obesity. *International Journal of Obesity*, *23*(2), S2–S11. https://doi.org/10.1038/sj.ijo.0800852

Naleid, A. M., Grace, M. K., Cummings, D. E., & Levine, A. S. (2005). Ghrelin induces feeding in the mesolimbic reward pathway between the ventral tegmental area and the nucleus accumbens. *Peptides*, *26*(11), 2274–2279. https://doi.org/https://doi.org/10.1016/j.peptides.2005.04.025

Neudorfer, C., Germann, J., Elias, G. J. B., Gramer, R., Boutet, A., & Lozano, A. M. (2020). A high-resolution in vivo magnetic resonance imaging atlas of the human hypothalamic region. *Scientific Data*, *7*(1), 305. https://doi.org/10.1038/s41597-020-00644-6

Ng, M., Fleming, T., Robinson, M., Thomson, B., Graetz, N., Margono, C., Mullany, E. C., Biryukov, S., Abbafati, C., Abera, S. F., Abraham, J. P., Abu-Rmeileh, N. M. E., Achoki, T., AlBuhairan, F. S., Alemu, Z. A., Alfonso, R., Ali, M. K., Ali, R., Guzman, N. A., … Gakidou, E. (2014). Global, regional, and national prevalence of overweight and obesity in children

and adults during 1980–2013: a systematic analysis for the Global Burden of Disease Study 2013. *The Lancet*, *384*(9945), 766–781. https://doi.org/10.1016/S0140-6736(14)60460-8

Palmer, C. E., Pecheva, D., Iversen, J. R., Hagler, D. J., Sugrue, L., Nedelec, P., Fan, C. C., Thompson, W. K., Jernigan, T. L., & Dale, A. M. (2022). Microstructural development from 9 to 14 years: Evidence from the ABCD Study. *Developmental Cognitive Neuroscience*, *53*, 101044. https://doi.org/https://doi.org/10.1016/j.dcn.2021.101044

Patenaude, B., Smith, S. M., Kennedy, D. N., & Jenkinson, M. (2011). A Bayesian model of shape and appearance for subcortical brain segmentation. *NeuroImage*, *56*(3), 907–922. https://doi.org/https://doi.org/10.1016/j.neuroimage.2011.02.046

Pistell, P. J., Morrison, C. D., Gupta, S., Knight, A. G., Keller, J. N., Ingram, D. K., & Bruce-Keller, A. J. (2010). Cognitive impairment following high fat diet consumption is associated with brain inflammation. *Journal of Neuroimmunology*, *219*(1–2), 25–32. https://doi.org/10.1016/j.jneuroim.2009.11.010

Power, J. D., Barnes, K. A., Snyder, A. Z., Schlaggar, B. L., & Petersen, S. E. (2012). Spurious but systematic correlations in functional connectivity MRI networks arise from subject motion. *NeuroImage*, *59*(3), 2142–2154. https://doi.org/10.1016/j.neuroimage.2011.10.018

Prieto, D., Contreras, C., & Sanchez, A. (2014). Endothelial Dysfunction, Obesity and Insulin Resistance. In *Current Vascular Pharmacology* (Vol. 12, Issue 3, pp. 412–426). https://doi.org/http://dx.doi.org/10.2174/1570161112666140423221008

R Core Team. (2013). *R: A language and environment for statistical computing*. R Foundation for Statistical Computing.

Raji, C. A., Ho, A. J., Parikshak, N. N., Becker, J. T., Lopez, O. L., Kuller, L. H., Hua, X., Leow, A. D., Toga, A. W., & Thompson, P. M. (2010). Brain structure and obesity. *Human Brain Mapping*, *31*(3), 353–364. https://doi.org/https://doi.org/10.1002/hbm.20870

Rapuano, K. M., Berrian, N., Baskin-Sommers, A., Décarie-Spain, L., Sharma, S., Fulton, S., Casey, B. J., & Watts, R. (2022). Longitudinal Evidence of a Vicious Cycle Between Nucleus Accumbens Microstructure and Childhood Weight Gain. *Journal of Adolescent Health*. https://doi.org/https://doi.org/10.1016/j.jadohealth.2022.01.002

Rapuano, K. M., Laurent, J. S., Hagler, D. J., Hatton, S. N., Thompson, W. K., Jernigan, T. L., Dale, A. M., Casey, B. J., & Watts, R. (2020). Nucleus accumbens cytoarchitecture predicts weight gain in children. *Proceedings of the National Academy of Sciences*, *117*(43), 26977–26984. https://doi.org/10.1073/pnas.2007918117

Robin, X., Turck, N., Hainard, A., Tiberti, N., Lisacek, F., Sanchez, J.-C., & Müller, M. (2011). pROC: an open-source package for R and S+ to analyze and compare ROC curves. *BMC Bioinformatics*, *12*(1), 77. https://doi.org/10.1186/1471-2105-12-77

Samara, A., Li, Z., Rutlin, J., Raji, C. A., Sun, P., Song, S.-K., Hershey, T., & Eisenstein, S. A. (2021). Nucleus accumbens microstructure mediates the relationship between obesity and eating behavior in adults. *Obesity*.

Samara, A., Murphy, T., Strain, J., Rutlin, J., Sun, P., Neyman, O., Sreevalsan, N., Shimony, J. S., Ances, B. M., Song, S. K., Hershey, T., & Eisenstein, S. A. (2020). Neuroinflammation and White Matter Alterations in Obesity Assessed by Diffusion Basis Spectrum Imaging. *Frontiers in Human Neuroscience*, *13*. https://doi.org/10.3389/fnhum.2019.00464

Schielzeth, H., Dingemanse, N. J., Nakagawa, S., Westneat, D. F., Allegue, H., Teplitsky, C., Réale, D., Dochtermann, N. A., Garamszegi, L. Z., & Araya-Ajoy, Y. G. (2020). Robustness of linear mixed-effects models to violations of distributional assumptions. *Methods in Ecology and Evolution*, *11*(9), 1141–1152. https://doi.org/https://doi.org/10.1111/2041-210X.13434

Schur, E. A., Melhorn, S. J., Oh, S.-K., Lacy, J. M., Berkseth, K. E., Guyenet, S. J., Sonnen, J. A., Tyagi, V., Rosalynn, M., De Leon, B., Webb, M. F., Gonsalves, Z. T., Fligner, C. L., Schwartz, M. W., & Maravilla, K. R. (2015). Radiologic evidence that hypothalamic gliosis is associated with obesity and insulin resistance in humans. *Obesity*, *23*(11), 2142–2148. https://doi.org/https://doi.org/10.1002/oby.21248

Sewaybricker, L. E., Kee, S., Melhorn, S. J., & Schur, E. A. (2021). Greater radiologic evidence of hypothalamic gliosis predicts adiposity gain in children at risk for obesity. *Obesity*, *29*(11), 1770–1779. https://doi.org/https://doi.org/10.1002/oby.23286

Sewaybricker, L. E., Melhorn, S. J., Papantoni, A., Webb, M. F., Hua, J., Roth, C. L., Carnell, S., & Schur, E. A. (2021). Pilot multi-site and reproducibility study of hypothalamic gliosis in children. *Pediatric Obesity*, *16*(4), e12732. https://doi.org/https://doi.org/10.1111/ijpo.12732

Sewaybricker, L. E., Schur, E. A., Melhorn, S. J., Campos, B. M., Askren, M. K., Nogueira, G. A. S., Zambon, M. P., Antonio, M. A. R. G. M., Cendes, F., Velloso, L. A., & Guerra-Junior, G. (2019). Initial evidence for hypothalamic gliosis in children with obesity by quantitative T2 MRI and implications for blood oxygen-level dependent response to glucose

ingestion. *Pediatric Obesity*, *14*(2), e12486. https://doi.org/https://doi.org/10.1111/ijpo.12486

Simmonds, M., Llewellyn, A., Owen, C. G., & Woolacott, N. (2016). Predicting adult obesity from childhood obesity: a systematic review and meta-analysis. *Obesity Reviews*, *17*(2), 95–107. https://doi.org/https://doi.org/10.1111/obr.12334

Skibicka, K. P., Hansson, C., Alvarez-Crespo, M., Friberg, P. A., & Dickson, S. L. (2011). Ghrelin directly targets the ventral tegmental area to increase food motivation. *Neuroscience*, *180*, 129–137. https://doi.org/https://doi.org/10.1016/j.neuroscience.2011.02.016

Smith, S. M., Jenkinson, M., Johansen-Berg, H., Rueckert, D., Nichols, T. E., Mackay, C. E., Watkins, K. E., Ciccarelli, O., Cader, M. Z., Matthews, P. M., & Behrens, T. E. J. (2006). Tract-based spatial statistics: Voxelwise analysis of multi-subject diffusion data. *NeuroImage*, *31*(4), 1487–1505. https://doi.org/https://doi.org/10.1016/j.neuroimage.2006.02.024

Smith, S. M., Jenkinson, M., Woolrich, M. W., Beckmann, C. F., Behrens, T. E. J., Johansen-Berg, H., Bannister, P. R., De Luca, M., Drobnjak, I., Flitney, D. E., Niazy, R. K., Saunders, J., Vickers, J., Zhang, Y., De Stefano, N., Brady, J. M., & Matthews, P. M. (2004). Advances in functional and structural MR image analysis and implementation as FSL. *NeuroImage*, *23*, S208–S219. https://doi.org/https://doi.org/10.1016/j.neuroimage.2004.07.051

Smith, S. M., & Nichols, T. E. (2009). Threshold-free cluster enhancement: Addressing problems of smoothing, threshold dependence and localisation in cluster inference. *NeuroImage*, *44*(1), 83–98. https://doi.org/https://doi.org/10.1016/j.neuroimage.2008.03.061

Sochocka, M., Diniz, B. S., & Leszek, J. (2017). Inflammatory Response in the CNS: Friend or Foe? *Molecular Neurobiology*, *54*(10), 8071–8089. https://doi.org/10.1007/s12035-016-0297-1

Spear, L. P. (2000). The adolescent brain and age-related behavioral manifestations. *Neuroscience & Biobehavioral Reviews*, *24*(4), 417–463. https://doi.org/https://doi.org/10.1016/S0149-7634(00)00014-2

Steven, A. J., Zhuo, J., & Melhem, E. R. (2013). Diffusion Kurtosis Imaging: An Emerging Technique for Evaluating the Microstructural Environment of the Brain. *American Journal of Roentgenology*, *202*(1), W26–W33. https://doi.org/10.2214/AJR.13.11365

Stice, E., Yokum, S., Burger, K. S., Epstein, L. H., & Small, D. M. (2011). Youth at Risk for Obesity Show Greater Activation of Striatal and Somatosensory Regions to Food. *The Journal of Neuroscience*, *31*(12), 4360 LP – 4366. https://doi.org/10.1523/JNEUROSCI.6604-10.2011

Stranahan, A. M., Hao, S., Dey, A., Yu, X., & Baban, B. (2016). Blood-brain barrier breakdown promotes macrophage infiltration and cognitive impairment in leptin receptor-deficient mice. *Journal of Cerebral Blood Flow and Metabolism : Official Journal of the International Society of Cerebral Blood Flow and Metabolism*, *36*(12), 2108–2121. https://doi.org/10.1177/0271678X16642233

Sun, P., George, A., Perantie, D. C., Trinkaus, K., Ye, Z., Naismith, R. T., Song, S.-K., & Cross, A. H. (2020). Diffusion basis spectrum imaging provides insights into MS pathology. *Neurology - Neuroimmunology Neuroinflammation*, *7*(2), e655. https://doi.org/10.1212/NXI.0000000000000655

Tait, J. L., Collyer, T. A., Gall, S. L., Magnussen, C. G., Venn, A. J., Dwyer, T., Fraser, B. J., Moran, C., Srikanth, V. K., & Callisaya, M. L. (2022). Longitudinal associations of childhood fitness and obesity profiles with midlife cognitive function: an Australian cohort study. *Journal of Science and Medicine in Sport*, *25*(8), 667–672. https://doi.org/https://doi.org/10.1016/j.jsams.2022.05.009

Thaler, J. P., Yi, C.-X., Schur, E. A., Guyenet, S. J., Hwang, B. H., Dietrich, M. O., Zhao, X., Sarruf, D. A., Izgur, V., Maravilla, K. R., Nguyen, H. T., Fischer, J. D., Matsen, M. E., Wisse, B. E., Morton, G. J., Horvath, T. L., Baskin, D. G., Tschöp, M. H., & Schwartz, M. W. (2012). Obesity is associated with hypothalamic injury in rodents and humans. *The Journal of Clinical Investigation*, *122*(1), 153–162. https://doi.org/10.1172/JCI59660

van Buuren, S., & Groothuis-Oudshoorn, K. (2011). mice: Multivariate Imputation by Chained Equations in R. *Journal of Statistical Software*, *45*(3 SE-Articles), 1–67. https://doi.org/10.18637/jss.v045.i03

Velloso, L. A., & Schwartz, M. W. (2011). Altered hypothalamic function in diet-induced obesity. In *International Journal of Obesity* (Vol. 35, Issue 12, pp. 1455–1465). https://doi.org/10.1038/ijo.2011.56

Wang, F., & Veugelers, P. J. (2008). Self-esteem and cognitive development in the era of the childhood obesity epidemic. *Obesity Reviews*, *9*(6), 615–623. https://doi.org/https://doi.org/10.1111/j.1467-789X.2008.00507.x

Wang, G. J., Volkow, N. D., Logan, J., Pappas, N. R., Wong, C. T., Zhu, W., Netusll, N., & Fowler, J. S. (2001). Brain dopamine and obesity. *Lancet*, *357*(9253), 354–357. https://doi.org/10.1016/S0140-6736(00)03643-6

Wang, Q., Wang, Y., Liu, J., Sutphen, C. L., Cruchaga, C., Blazey, T., Gordon, B. A., Su, Y., Chen, C., Shimony, J. S., Ances, B. M., Cairns, N. J., Fagan, A. M., Morris, J. C., & Benzinger, T. L. S. (2019). Quantification of white matter cellularity and damage in preclinical and early symptomatic Alzheimer's disease. *NeuroImage. Clinical*, *22*, 101767. https://doi.org/10.1016/j.nicl.2019.101767

Wang, X., Cusick, M. F., Wang, Y., Sun, P., Libbey, J. E., Trinkaus, K., Fujinami, R. S., & Song, S.-K. (2014). Diffusion basis spectrum imaging detects and distinguishes coexisting subclinical inflammation, demyelination and axonal injury in experimental autoimmune encephalomyelitis mice. *NMR in Biomedicine*, *27*(7), 843–852. https://doi.org/https://doi.org/10.1002/nbm.3129

Wang, Y., Sun, P., Wang, Q., Trinkaus, K., Schmidt, R. E., Naismith, R. T., Cross, A. H., & Song, S. K. (2015). Differentiation and quantification of inflammation, demyelination and axon injury or loss in multiple sclerosis. *Brain*, *138*(5), 1223–1238. https://doi.org/10.1093/brain/awv046

Wang, Y., Wang, Q., Haldar, J. P., Yeh, F.-C., Xie, M., Sun, P., Tu, T.-W., Trinkaus, K., Klein, R. S., Cross, A. H., & Song, S.-K. (2011). Quantification of increased cellularity during inflammatory demyelination. *Brain : A Journal of Neurology*, *134*(Pt 12), 3590–3601. https://doi.org/10.1093/brain/awr307

White, N. S., Leergaard, T. B., D'Arceuil, H., Bjaalie, J. G., & Dale, A. M. (2013). Probing tissue microstructure with restriction spectrum imaging: Histological and theoretical validation. *Human Brain Mapping*, *34*(2), 327–346. https://doi.org/https://doi.org/10.1002/hbm.21454

Winkler, A. M., Ridgway, G. R., Webster, M. A., Smith, S. M., & Nichols, T. E. (2014). Permutation inference for the general linear model. *NeuroImage*, *92*, 381–397. https://doi.org/https://doi.org/10.1016/j.neuroimage.2014.01.060

Wu, C., Garamszegi, S. P., Xie, X., & Mash, D. C. (2017). Altered Dopamine Synaptic Markers in Postmortem Brain of Obese Subjects . In *Frontiers in Human Neuroscience* (Vol. 11, p. 386). https://www.frontiersin.org/article/10.3389/fnhum.2017.00386

Yang, R., Lin, T.-H., Zhan, J., Lai, S., Song, C., Sun, P., Ye, Z., Wallendorf, M., George, A., Cross, A. H., & Song, S.-K. (2021). Diffusion basis spectrum imaging measures anti-inflammatory and neuroprotective effects of fingolimod on murine optic neuritis. *NeuroImage. Clinical*, *31*, 102732. https://doi.org/10.1016/j.nicl.2021.102732

Ye, Z., Gary, S. E., Sun, P., Mustafi, S. M., Glenn, G. R., Yeh, F.-C., Merisaari, H., Song, C., Yang, R., Huang, G.-S., Kao, H.-W., Lin, C.-Y., Wu, Y.-C., Jensen, J. H., & Song, S.-K. (2021). The impact of edema and fiber crossing on diffusion MRI metrics assessed in an ex vivo nerve phantom: Multi-tensor model vs. diffusion orientation distribution function. *NMR in Biomedicine*, *34*(1), e4414. https://doi.org/https://doi.org/10.1002/nbm.4414

Yendiki, A., Koldewyn, K., Kakunoori, S., Kanwisher, N., & Fischl, B. (2014). Spurious group differences due to head motion in a diffusion MRI study. *NeuroImage*, *88*, 79–90. https://doi.org/10.1016/j.neuroimage.2013.11.027

Zhan, J., Lin, T.-H., Libbey, J. E., Sun, P., Ye, Z., Song, C., Wallendorf, M., Gong, H., Fujinami, R. S., & Song, S.-K. (2018). Diffusion Basis Spectrum and Diffusion Tensor Imaging Detect Hippocampal Inflammation and Dendritic Injury in a Virus-Induced Mouse Model of Epilepsy . In *Frontiers in Neuroscience* (Vol. 12, p. 77). https://www.frontiersin.org/article/10.3389/fnins.2018.00077

Zhang, H., Schneider, T., Wheeler-Kingshott, C. A., & Alexander, D. C. (2012). NODDI: Practical in vivo neurite orientation dispersion and density imaging of the human brain. *NeuroImage*, *61*(4), 1000–1016. https://doi.org/https://doi.org/10.1016/j.neuroimage.2012.03.072

Variable	Group			*p*-value
	NW (*n* = 126)	**OW** (*n* = 64)	**OB** (*n* = 68)	
Age (month)	121 ± 7	121 ± 7	119 ± 8	0.31
Sex				
Male	66 (52.4%)	34 (53.1%)	33 (48.5%)	0.84
Female	60 (47.6%)	30 (46.9%)	35 (51.5%)	
Race/ethnicity				
Asian	3 (2.4%)	0 (0%)	2 (2.9%)	
Black	8 (6.3%)	9 (14.1%)	10 (14.7%)	0.03 *
Hispanic	16 (12.7%)	14 (21.9%)	17 (25.0%)	
White	90 (71.4%)	35 (54.7%)	31 (45.6%)	
Other	9 (7.1%)	6 (9.4%)	8 (11.8%)	
PDS category				
1	81 (64.3%)	25 (39.1%)	27 (39.7%)	0.003 **
2	26 (20.6%)	14 (21.9%)	18 (26.5%)	
3+	19 (15.1%)	25 (39.1%)	23 (33.8%)	
Parental education				
No HS diploma	3 (2.4%)	4 (6.2%)	2 (2.9%)	
HS diploma/ GED	2 (1.6%)	2 (3.1%)	5 (7.4%)	0.001 **
Some college	24 (19.0%)	21 (32.8%)	29 (42.6%)	
Bachelor	40 (31.7%)	16 (25.0%)	12 (17.6%)	
Postgraduate	57 (45.2%)	21 (32.8%)	20 (29.4%)	
Household income‡				
< 50k	13 (10.3%)	20 (31.2%)	17 (25.0%)	< 0.001 ***
≥ 50k & < 100k	39 (31.0%)	16 (25.0%)	21 (30.9%)	
≥ 100k	74 (58.7%)	28 (43.8%)	30 (44.1%)	
Parental marriage				
Married	102 (81.0%)	44 (68.8%)	45 (66.2%)	< 0.001 ***
Not married	24 (19.0%)	20 (31.2%)	23 (33.8%)	
Mean motion (mm)	1.20 ± 0.21	1.22 ± 0.25	1.28 ± 0.28	0.08
ICV (mm^3)	1573519 ± 136795	1579465 ± 147127	1594320 ± 129161	0.60
$V_{hypothalamus}$ (mm^3)	737 ± 95	719 ± 92	733 ± 92	0.47
$V_{nucleus\ accumbens}$ (mm^3)	1044 ± 208	998 ± 231	1042 ± 209	0.34
$V_{caudate\ nucleus}$ (mm^3)	7889 ± 1040	7885 ± 1115	7974 ± 933	0.79
$V_{putamen}$ (mm^3)	10642 ± 1278	10268 ± 1197	10643 ± 1119	0.10
Obesity-related measures				
Baseline				
BMI (kg/m^2)	16.84 ± 1.50	20.99 ± 0.82	25.35 ± 2.73	< 0.001 ***
BMI percentile	47.92 ± 23.54	90.52 ± 2.78	97.24 ± 1.47	< 0.001 ***
BMI *z*-score	-0.07 ± 0.69	1.34 ± 0.17	1.99 ± 0.27	< 0.001 ***
WC (inch)	25.14 ± 2.25	29.11 ± 2.40	32.91 ± 3.71	< 0.001 ***
One-year				
BMI (kg/m^2)	17.52 ± 1.96	21.71 ± 2.14	26.67 ± 3.91	< 0.001 ***
BMI *z*-score	-0.07 ± 0.79	1.22 ± 0.46	1.95 ± 0.39	< 0.001 ***
WC (in) †	25.83 ± 2.40	30.06 ± 2.67	34.45 ± 4.17	< 0.001 ***
Change (Δ) over one year				
ΔBMI (kg/m^2)	0.68 ± 1.09	0.71 ± 1.87	1.32 ± 2.25	0.03 *
ΔBMI *z*-score	-0.01 ± 0.42	-0.12 ± 0.44	-0.05 ± 0.31	0.19
ΔWC (in) †	0.70 ± 2.05	0.95 ± 2.72	1.54 ± 3.05	0.08
Two-year				
BMI (kg/m^2) †	18.39 ± 2.21	23.10 ± 2.92	28.03 ± 4.20	< 0.001 ***
BMI *z*-score†	0.00 ± 0.88	1.29 ± 0.52	1.96 ± 0.49	< 0.001 ***
WC (in) †	27.28 ± 3.01	31.61 ± 3.29	36.67 ± 4.80	< 0.001 ***
Change (Δ) over two years				
ΔBMI (kg/m^2) †	1.55 ± 1.51	2.09 ± 2.66	2.70 ± 3.00	0.004 **
ΔBMI *z*-score†	0.06 ± 0.61	-0.05 ± 0.49	-0.03 ± 0.45	0.30
ΔWC (in) †	2.13 ± 2.61	2.45 ± 3.20	3.22 ± 3.63	0.06

Table 1. Participant demographics, brain volumes, and obesity-related measures. Continuous variables reported as mean ± SD. Categorical variables reported as count (percentage). Variables are baseline unless otherwise noted. One-way ANOVA and Pearson's chi-squared tests were used as appropriate. Data from five participants with underweight are not shown and were not included in comparisons due to small group size. Abbreviations: NW, children with normal weight; OW, with overweight; OB, with obesity; PDS, pubertal development scale; HS, high school; GED, General Educational Development; ICV, intracranial volume; BMI, body mass index; WC, waist circumference. †, one NW participant had one-year WC removed due to extreme value; one NW participant, two OW participants, and one OB participant had missing two-year BMI, BMI *z*-score, and WC; additionally, another OB participant had missing two-year WC. Pairwise deletion was applied in relevant analyses. ‡, 20 missing entries were imputed. *, $p \leq 0.05$; **, $p \leq 0.01$; ***, $p \leq 0.001$.

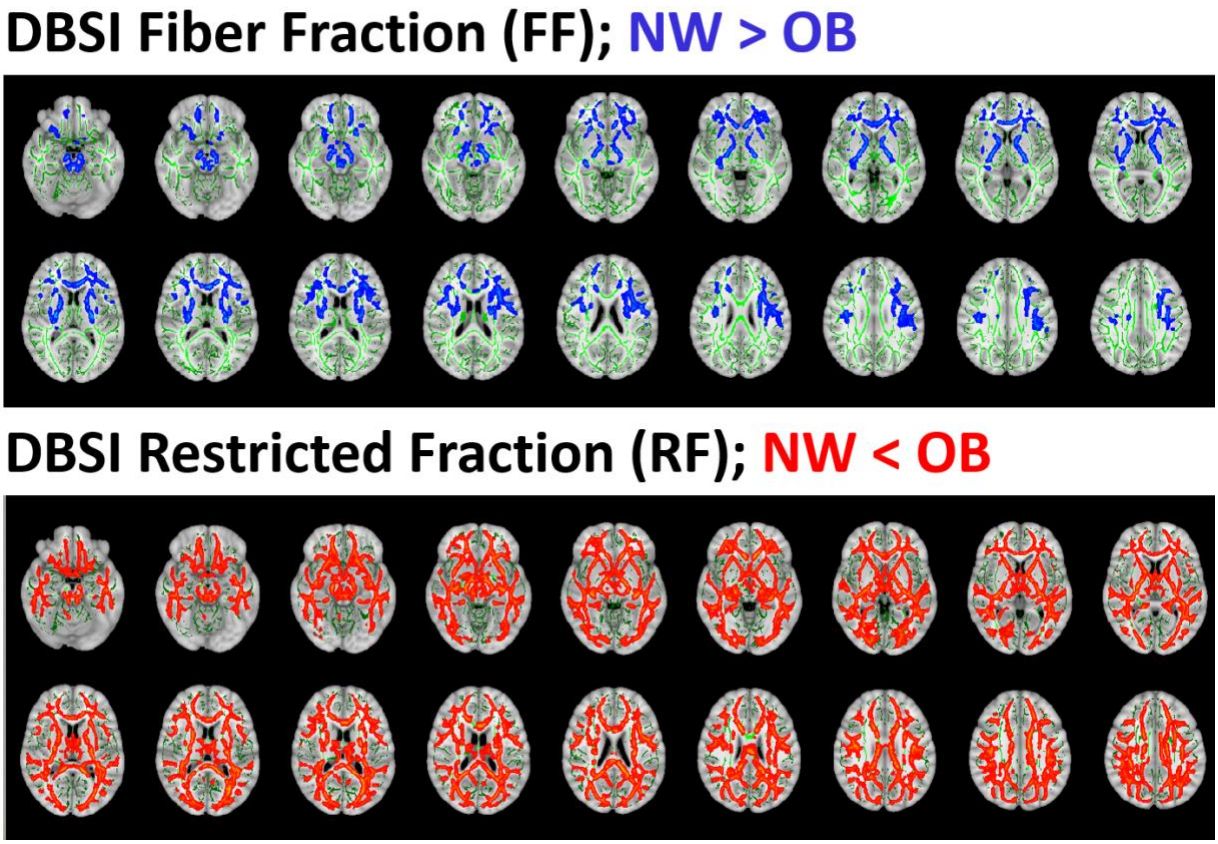

Fig. 1. (2-column, with color) Voxel-wise comparisons of white matter (WM) DBSI metrics between children with normal-weight (NW; n = 126) and obesity (OB; n = 68). For each metric, axial images range from most ventral (top left) to most dorsal (bottom right). *Green*: WM skeleton; *Blue, light blue*: NW > OB at FWE-corrected $p \leq 0.05$, 0.01; *Red, yellow*: NW < OB at FWE-corrected $p \leq 0.05$, 0.01. Analyses controlled for age, sex, race/ethnicity, parental education, pubertal development scale scores, and mean head motion. DBSI, diffusion basis spectrum imaging.

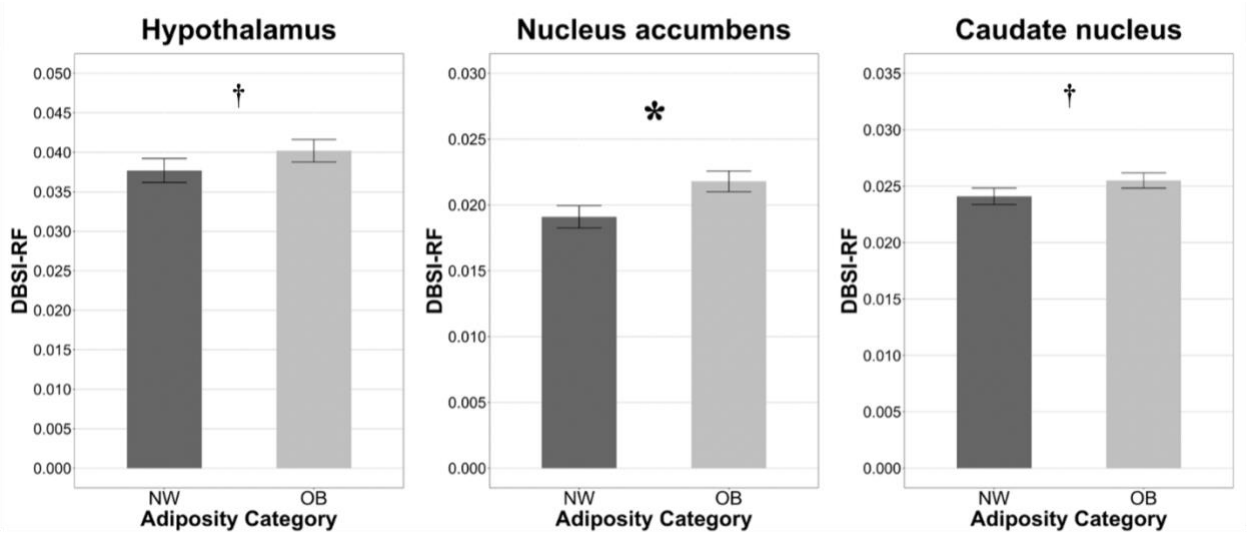

Fig. 2. (2-column, greyscale) Comparisons of DBSI-RF in the hypothalamus and striatum between children with normal-weight (NW; n = 126) and obesity (OB; n = 68). Bars represent group means ± standard error, adjusted for age, sex, race/ethnicity, parental education, pubertal development scale scores, mean head motion, and intracranial volume. Detailed statistics shown in **Table 2**. DBSI, diffusion basis spectrum imaging; RF, restricted fraction. *, $p \leq 0.0125$. †, nominally significant but did not pass multiple comparison correction.

ROI	Metric	Adjusted mean (SE)		*p*-value	Cohen's *d* (95% CI)
		NW (*n* = 126)	OB (*n* = 68)		
Hypothalamus	DBSI-FF	0.528 (0.006)	0.526 (0.006)	0.66	-0.08 (-0.37 – 0.22)
	DBSI-RF	0.037 (0.002)	0.040 (0.001)	0.0503 †	0.31 (0.02 – 0.61)
Nucleus accumbens	DBSI-FF	0.411 (0.007)	0.410 (0.006)	0.78	-0.02 (-0.31 – 0.27)
	DBSI-RF	0.019 (0.001)	0.022 (0.001)	0.0001 *	0.55 (0.25 – 0.85)
Caudate nucleus	DBSI-FF	0.363 (0.005)	0.361 (0.004)	0.57	-0.07 (-0.36 – 0.23)
	DBSI-RF	0.024 (0.001)	0.026 (0.001)	0.0223 †	0.28 (-0.01 – 0.58)
Putamen	DBSI-FF	0.392 (0.004)	0.390 (0.003)	0.72	-0.03 (-0.33 – 0.26)
	DBSI-RF	0.032 (0.001)	0.033 (0.001)	0.26	0.12 (-0.17 – 0.42)

Table 2. Comparison of DBSI metrics in the hypothalamus and striatum between children with normal-weight (NW, $n = 126$) and obesity (OB, $n = 68$). ROI, region of interest; SE, standard error; CI, confidence interval; DBSI, diffusion basis spectrum imaging; FF, fiber fraction; RF, restricted fraction. †, $p \leq 0.05$; *, $p \leq 0.0125$. Significant results are visualized in **Fig. 2**.

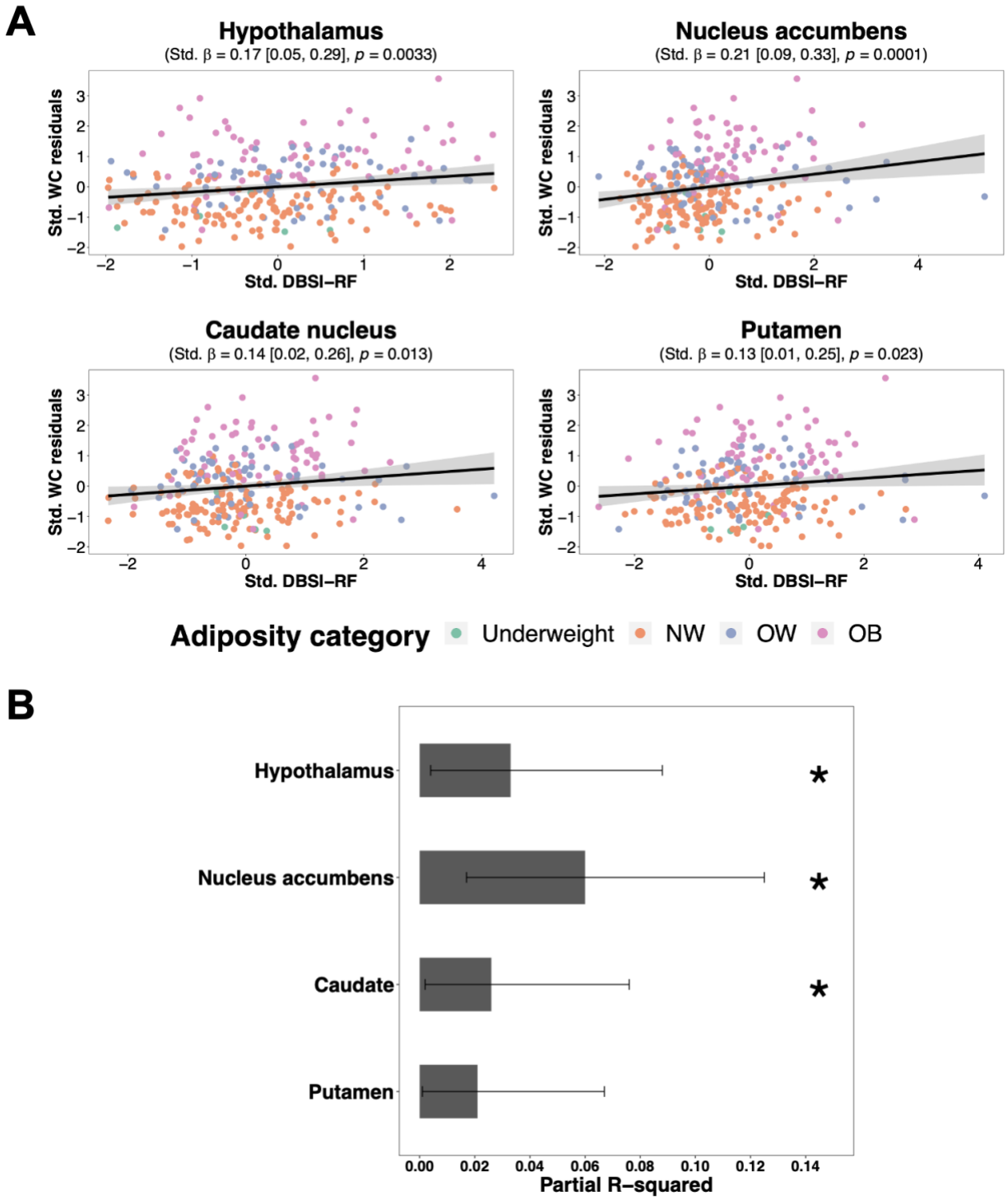

Fig. 3. (2-column, with color) Associations between baseline waist circumference (WC) and DBSI-RF in the hypothalamus and striatum in all children (*n* = 263). **(A)** WC residuals (accounting for age, sex, race/ethnicity, puberty development scale, parental education, household income, parental marital status, mean head motion, intracranial volume, and scanning site) and DBSI-RF normalized to *z*-scores.

Standardized (Std.) β regression coefficients were reported with 95% confidence intervals (shaded regions). BMI, body mass index; NW, children with normal-weight; OW, children with over-weight; OB, children with obesity. **(B)** Partial R^2 of WC explained by DBSI-RF in regions. DBSI, diffusion basis spectrum imaging; RF, restricted fraction. *, $p \leq 0.0125$.

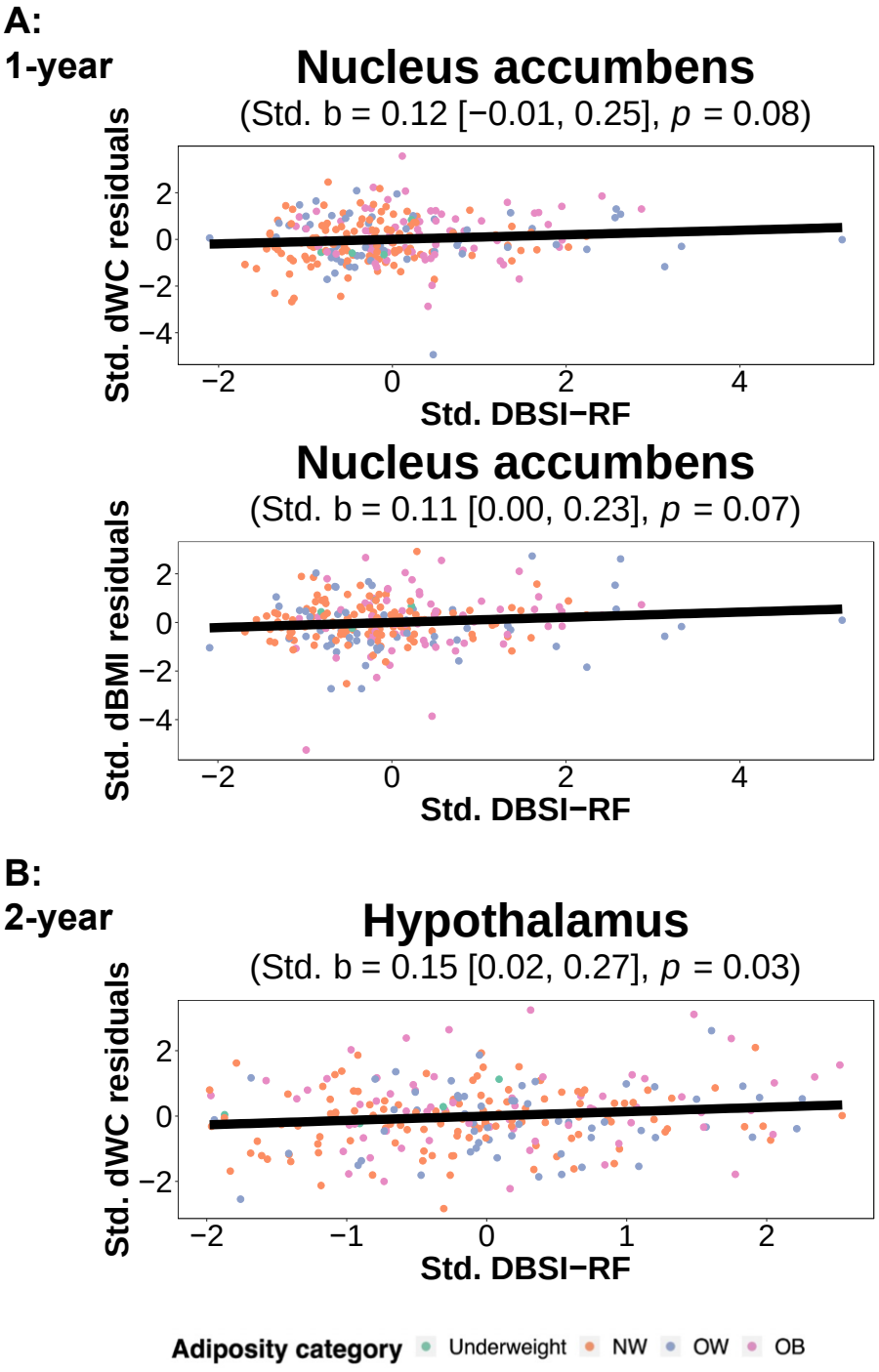

Fig. 4. (1-column, with color) (**A**) Associations between DBSI-RF in the nucleus accumbens and **one-year change** (d) in waist circumference (WC; *top*, n = 250) and body mass index (BMI; *bottom*, n = 251). (**B**) Association between DBSI-RF in the hypothalamus and **two-year change** in WC (n = 247). All associations accounted for the corresponding baseline obesity-related measure. Standardized (Std.) β regression coefficients were reported with 95% confidence intervals (shaded regions). DBSI, diffusion basis spectrum imaging; RF, restricted fraction; NW, children with normal-weight; OW, children with over-weight; OB, children with obesity.

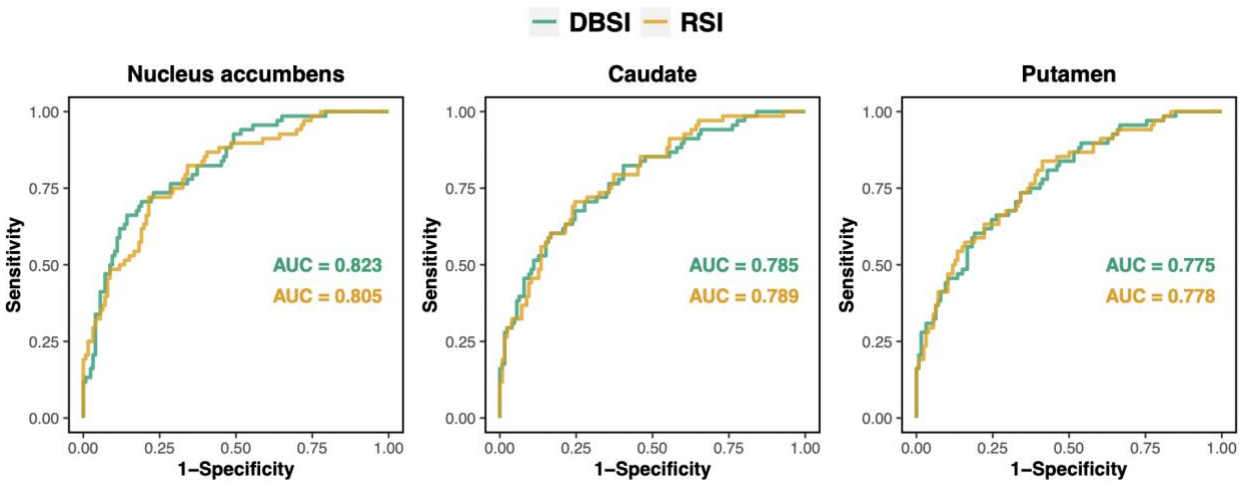

Fig. 5 (2-column, with color) Receiver operating characteristic curves comparing DBSI and RSI models in classifying children with normal-weight (*n* = 126) and obesity (*n* = 68). For DBSI, DBSI-RF was used. For RSI, restricted isotropic component was used. AUC, area-under-the-curve; DBSI, diffusion basis spectrum imaging; RSI, restriction spectrum imaging.